Science of the Total Environment 830 (2022) 154706

Contents lists available at ScienceDirect

Science of the Total Environment

journal homepage: www.elsevier.com/locate/scitotenv

Rare earth elements and yttrium as tracers of waste/rock-groundwater interactions

Dioni I. Cendón [a,b,*], Brett Rowling [a], Catherine E. Hughes [a], Timothy E. Payne [a], Stuart I. Hankin [a], Jennifer J. Harrison [a], Mark A. Peterson [a], Attila Stopic [a], Henri Wong [a], Patricia Gadd [a]

[a] Australian Nuclear Science and Technology Organisation, Lucas Heights, NSW 2234, Australia
[b] School of Biological, Earth and Environmental Sciences, UNSW Sydney, NSW, 2052, Australia

HIGHLIGHTS

- Waste-groundwater interactions are studied using Rare Earth elements and Yttrium (REY)
- Groundwater Gd, Eu, Sm enrichments are linked to low-level radioactive waste
- Urban leachate shows different REY enrichments to local geology and radioactive waste
- REY trace groundwater pollution sources in co-located urban and radioactive disposal sites
- During groundwater recharge, REY evolve with landfill leachate, waste and rock interactions

GRAPHICAL ABSTRACT

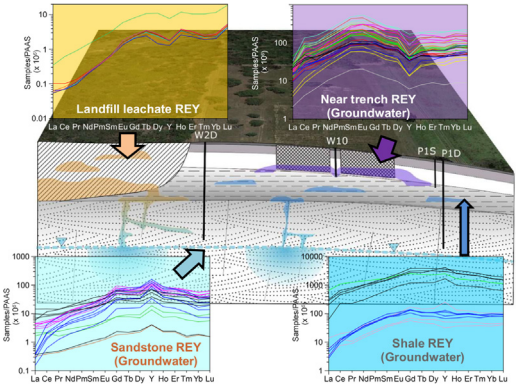

ARTICLE INFO

Article history:
Received 27 January 2022
Received in revised form 3 March 2022
Accepted 16 March 2022
Available online 21 March 2022

Editor: Jurgen Mahlknecht

Keywords:
Rare earth elements and yttrium (REY)
Landfill
Low-level nuclear waste
Waste-rock interaction
Tritium
Little Forest Legacy Site

ABSTRACT

Increasing concentrations of Rare Earth Elements (REE) plus yttrium (REY) are entering the environment due to human activities. The similar chemical behaviour across the whole REY, i.e. the lanthanide series (lanthanum to lutetium) and yttrium, allows their use as tracers, fingerprinting rock-forming processes and fluid-rock interactions in earth science systems. However, their use in fingerprinting waste and particularly low-level radioactive waste has not received much attention, despite the direct use of REE in the nuclear industry and the traditional use of REE as proxies to understand the environmental mobility of the actinide series (actinium to lawrencium). The highly instrumented low-level radioactive waste site at Little Forest (Australia) allows a detailed REY study, investigating interactions with local strata, neighbouring waste forms and shallow groundwater flows. Groundwater samples and solids from cored materials were recovered from 2007 to 2012 from the study site and regional baseline sites in the same geological materials. The REY in water samples were analysed by automated chelation pre-concentration (SeaFast, ESI) followed by ICP-MS determination, while solid samples were analysed using Neutron Activation Analysis (NAA) and X-ray fluorescence scanning (ITRAX). Solid rocks showed no REY departed from typical Upper Crust compositions in either Little Forest or regional background sites. Shallow groundwater from ~4–5 m, at or slightly below waste trench levels, showed water-waste interaction as a marked enrichment, relative to shale-normalised patterns, in samarium, europium and gadolinium, with depleted yttrium. Leachate samples from the neighbouring urban landfill show different REY normalised patterns. REY distribution changes with depth through increased interaction with shales and sandstones. Variations in pH and redox conditions lead to widespread precipitation of Fe-hydroxides, which scavenge REY with differential uptake by precipitating solids, resulting in increases in Y and higher Y/Ho ratio in the groundwater along the flow path. Our study revealed that the Little Forest low-level radioactive waste has a REY fingerprint

* Corresponding author at: Australian Nuclear Science and Technology Organisation, Lucas Heights, NSW 2234, Australia.
E-mail address: dce@ansto.gov.au (D.I. Cendón).

http://dx.doi.org/10.1016/j.scitotenv.2022.154706

different to that of groundwater in surrounding land uses. REY can be used to fingerprint diverse waste sources, assess the mobility of lanthanides inferring the mobility of selected actinides, and to trace the fate of REY during groundwater recharge. The approach presented can refine source allocation and trace pollutant mobility in current and legacy urban, mixed and radioactive waste sites around the world.

1. Introduction

The not so "rare" earth elements and yttrium are a group of strategic metals more abundant than metals like gold, silver, bismuth or cadmium (Rudnick et al., 2003). The increasing number of applications, particularly in cutting edge electronics (magnets, wind turbines, batteries), has seen their demand soaring in the last decade and they are currently listed as critical elements by the US government (Federal Register, 2018). The increasing application of REY has opened new pathways for their dispersion into the environment, particularly in specific industrial activities such as mining, metallurgy, agriculture, health diagnostics and waste management (e.g.: Borrego et al., 2004; Loell et al., 2011).

The efficacy of REY as tracers of elemental provenance and interactions in rocks and fluids has been long recognised in earth science systems (Nance and Taylor, 1976; Olivarez and Owen, 1991; Nozaki et al., 1997; Wyndham et al., 2004; Hathorne et al., 2012; amongst many others). An increasing number of studies have also characterised REY in surface water (Möller and Bau, 1993; Lawrence et al., 2006) and groundwater (Möller et al., 2003; Johannesson, 2005; Tweed et al., 2006; Duvert et al., 2015). For example, Bau and Dulski (1996), observed positive gadolinium anomalies in surface waters and linked them to its use as contrast agent in magnetic resonance imaging and ultimately to hospital sewage. More recently Hissler et al. (2016) studied the input of anthropogenic REE and historical pollution sources in dissolved and suspended loads of the Alzette River (Luxembourg). However, REY's potential to differentiate waste provenance or integrity at contaminated sites has received little attention.

Despite the potential of REY as tracers, several factors have hindered their wider use: A) generally low dissolved concentrations (~ng L^{-1}); B) their non-conservative nature during mineral precipitation of common low-temperature/regolith minerals (Fe-Mn-oxyhydoxides, phosphates, carbonates); C) complex water-rock/waste interaction processes (Bau, 1999; Leybourne and Johannesson, 2008); and D) the affinity of REY to be complexed by organic substances (Tang and Johannesson, 2010; Stolpe et al., 2013). However, these perceived limitations can lead to additional insights when improved analytical techniques are combined with REY assessments along flow paths.

For the nuclear industry, the systematics of REY distributions offer the potential to fingerprint radioactive waste and/or assess waste repository integrity. This application would be in addition to the common use of rare earths (Nd^{3+}, Eu^{3+}) as proxy elements for trivalent actinides such as Pu^{3+} or Am^{3+}; REY being key elements in nuclear reactors to regulate neutron flux and REY co-existing within the UTh ores and waste (Ray, 1971; Krauskopf, 1986; Johannesson and Stetzenbach, 1995; Ewing, 1999; Missana et al., 2008; Balboni et al., 2017).

In this study we characterise the REY distribution in groundwater at a low-level radioactive waste site situated in the urban fringes of Sydney (Australia). There are other sources of groundwater contaminants surrounding the site, including an unlined municipal landfill, disposal of industrial liquid contaminants and solid human waste ("night soils"). We aim to: A) characterise groundwater REY in the proximity of radioactive waste trenches to determine whether this specific source can be differentiated from that of groundwater interacting with other waste sources around the site, and B) qualitatively assess vertical and horizontal integrity of the site by comparing REY beyond the waste enclosed area. This research is intended to evaluate the usefulness of REY as tracers of groundwater-waste interactions and determine whether this methodology can be employed in other waste sites worldwide to test potential transport of pollutants or test the geological isolation of a site.

2. Background and study site

2.1. Rare earth elements and yttrium systematics

Rare Earth Elements (REE) are part of the inner transition metals, forming a group of 15 elements (Peters et al., 2020). Yttrium is generally included (REY) due to it having similar characteristics to holmium, generally referred to as yttrium's twin element (Pack et al., 2007). The REEs exhibit a gradual decrease in ionic radii with increasing atomic number from La through Lu (lanthanide contraction) despite their uniform oxidation state (+3) except for Ce and Eu that can also attain a +4 and +2 oxidation state respectively. Their similar masses, ionic radii and oxidation states lead to similar chemical behaviour for the whole series. This behaviour is better appreciated when concentrations are normalised against their average abundance. In environmental studies REY are generally normalised against their respective upper crust abundance. For example, Post Archean Australian Shale (PAAS) incorporates the REY composition of large regions with diverse geology (Nance and Taylor, 1976; Pourmand et al., 2012). The resulting normalised patterns (sample concentration/average composite) plotted against atomic number and/or REY radii, can help to visualise anomalies compared to their neighbouring elements (enrichments and depletions). These anomalies can be calculated using different equation schemes (e.g.: Lawrence et al., 2006). In this paper, at least otherwise stated, we calculate REY enrichments and depletions using shale-normalised patterns. The calculated relative variations can then be interpreted as differences in sources and/or processes. In this study we differentiate REE's into light or LREE (La to Pm), middle or MREE (Sm to Dy) and heavy or HREE (Ho to Lu). The normalised concentrations are generally denoted as the element with a subscript N (eg.: Eu_N). In this paper we adopt the revised PAAS values of Pourmand et al. (2012) for concentration normalisation.

2.2. Site physiography and geology

The Little Forest Legacy Site (LFLS) is a 5.5 ha fenced area ~ 1.6 km north of the Lucas Heights Science and Technology Centre (Sydney, Australia). The disposal area is situated on a hydrologic divide between two creeks (Fig. 1). The hydrogeological characteristics of the site, potential transport-flowpaths and waste disposal history have been described in Hughes et al. (2011); Payne et al. (2013); Cendón et al. (2015) and Payne et al. (2020), and the reader is referred to those sources for details.

In summary, dominant lithologies outcropping in the area are of Triassic age and consist of the Hawkesbury Sandstone, which extends to a depth of at least 192 m and regionally across the Sydney Basin. Laterally discontinuous shale lenses are interbedded within the sandstone. It is within one of those shale lenses that the LFLS site is located. The shale lens dips towards the northeast and is closer to the surface in the southern area of the site. The maximum thickness of the shale lens is ~14 m and thins to as little as 4 m on the south eastern boundary of the site with sandstone outcropping outside the fenced perimeter.

The soils at the site are highly weathered and derived from the shale, resulting in a profile ranging from surficial red–brown clay soil, through mottled grey, silty kaolinite clay with numerous fine sandy partings. Immediately below the weathered material lies a light-grey leached silty shale grading to fresh dark carbonaceous parent shale with silty interbeddings (Fig. 1 Supplementary). The parent shale grades into shale/sandstone laminae above the basal Hawkesbury Sandstone. The underlying Hawkesbury Sandstone consists primarily of laterally discontinuous quartzose sandstone units ranging in thickness from 1.5 m to 3.0 m, with some siltstone/fine

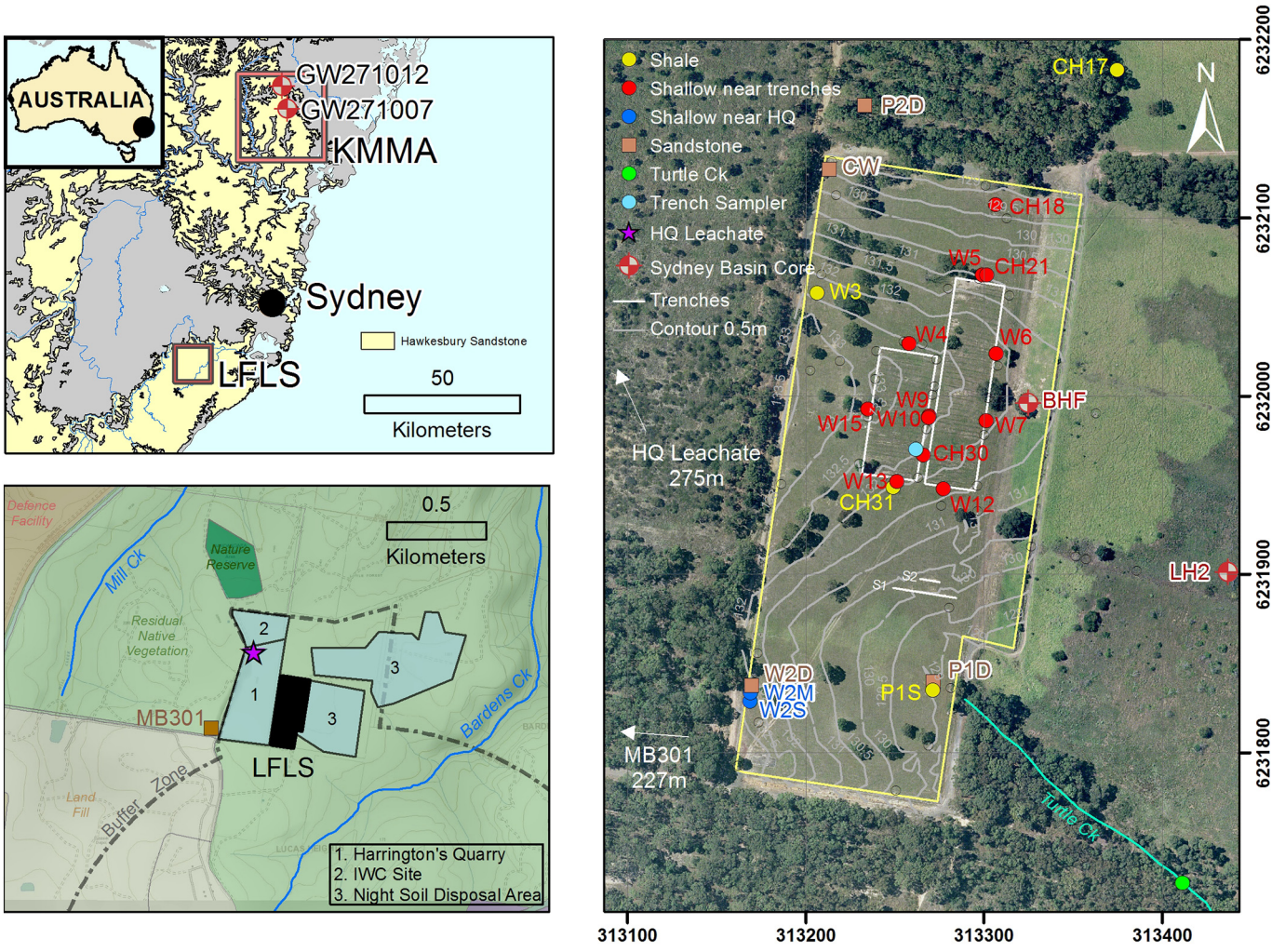

Fig. 1. (a) General location of the Little Forest Legacy Site (LFLS) and regional background groundwater and solid samples from the Kulnura-Mangrove Mountain Aquifer (KMMA). For detailed location of the regional background sites see Cendón et al. (2014). (b) Land use surrounding the LFLS and location of some monitoring wells outside the detailed area. (c) Satellite photograph of the LFLS site with trench location (white rectangles), surface contours and types of monitoring wells or sampling points.

sandstone laminae, siltstone and claystone interbeds. The sandstone is composed mostly of medium grain sand cemented with silica, clay and iron oxides or carbonates.

2.3. Climate and hydrogeology

The LFLS area has a humid subtropical climate (Köppen climate classification Cfa) with maritime influences. Mean annual rainfall at Lucas Heights (BOM Station 066078) was 999 mm for the period 1959–2019 with annual average pan evaporation being ~1200 mm. The period during which sampling for this study occurred experienced average rainfall but was preceded by a lengthy drought from 2000 to 2006.

Cores of weathered shale extracted from below and adjacent to the trenches have typically been unsaturated (Fig. 1 Supplementary), with variable levels of moisture in perched horizons that appear to be discontinuous across the site (Hankin, 2012). Periodic infiltration and lateral movement along perched horizons within the vadose zone have led to standing water accumulating in site wells. In general, most shallow wells within the vadose zone exhibit water level increases immediately following large precipitation events, indicating a clear connection to the surface via infiltration. Deeper wells show a parallel but dampened response compared to shallow wells (Hughes et al., 2011).

The parent shale is expected to minimise direct downward movement of groundwater into the Hawkesbury Sandstone below. Springs related to the transition between the shale–sandstone emerge at the limits of the shale outcrop southeast of LFLS particularly along Turtle Creek (shown in Fig. 1c). The Hawkesbury Sandstone has been generalised as a layered aquifer system with groundwater occurring in discrete horizons with occasional vertical connection (McKibbin and Smith, 2000). The local hydrological regime of the LFLS has been modified by various land uses.

2.4. Waste disposal at LFLS and neighbouring sites

An estimated total of 1675 m^3 of waste was disposed of in 79 trenches at LFLS between 1960 and 1968 (Isaacs and Mears, 1977). The trenches were 3 m deep and located within the two rectangles shown in Fig. 1c (see Payne (2012) for details). The uncompacted waste was placed above a shale layer approximately ~7 m thick and subsequently covered by mixed soil (~1 m) from trench excavation. The total activity of radionuclides is indicated by records to be ~150 GBq at the time of disposal (AAEC, 1985; Payne, 2012). A major proportion of activity in the waste comprised short-lived isotopes including ^{60}Co and ^{137}Cs and ^{90}Sr. However, the waste also included longer-lived isotopes including actinides, specifically several grams of $^{239+240}Pu$, ^{233}U and ^{235}U and larger amounts of ^{238}U and ^{232}Th. The tritium amount disposed of was estimated at ~4 TBq and is believed to have been derived from operations of the HIFAR reactor (Hughes et al., 2011). Disposal records indicate the disposal of several hundred waste drums containing residues from the processing and subsequent drying of sludge. Some ~1070 kg of beryllium related to reactor design investigations were also disposed of at the site (AAEC, 1985).

The neighbouring areas around the LFLS site have had diverse land uses and the reader is referred to Payne et al. (2013) and Cendón et al. (2015) for details. In summary, disposal of industrial chemicals took place at the Industrial Waste Collection Pty Ltd. (IWC) Liquid Waste Depot, approximately 400 m NW of LFLS between 1969 and 1980 (Coffey Partners International Pty Ltd, 1991). Disposal was concentrated in the excavations left by shale quarries and prospects. The area directly adjacent and ENE of LFLS was used for the disposal of household organic waste or "night soils" (pit latrines) from 1947 to 1990.

Bordering the site along the west, approximately 6 ha were excavated for shale and sandstone at Harrington's Quarry between the mid-1950s and 1980s (Coffey Partners International Pty Ltd, 1991; GHD 2003). Excavations were deeper on the northern side of the quarry, where they reached 7 m below surface, and progressively shallower to the south where the shale layer was closer to surface. Harrington's Quarry was filled with 450,000–600,000 t of municipal waste in 1987. No clay seal was installed at the base of the landfill, with waste in direct contact with the underlying sandstone. A leachate drainage and pump-out system were installed prior to filling the area. However, the leachate sump is not located at the deepest section, therefore leachate derived from the waste material, particularly in the northern section, may not be effectively removed (GHD 2003). Leachate pumped between 2005 and 2008 averaged 9.7 $m^3 \cdot day^{-1}$.

3. Sampling and analytical methods

The LFLS has a comprehensive network of shallow groundwater monitoring wells. The initial monitoring well network consisted mostly of non-screened or long-screened wells (here "long-screen" means a screen without separation of specific water-bearing zones) with construction characteristics evolving since the late 1950s (Hughes et al., 2011; Hankin, 2012; Cendón et al., 2015). Groundwater samples were recovered from available infrastructure from 2007 to 2012. Sampling from older monitoring wells was progressively phased out as new short-screened wells became available. In this paper we provide all available results, while interpretations rely on short-screened monitoring wells with increased availability for the 2010–2012 period (Table 1, Supplementary). Additionally, we recovered samples from a groundwater discharge point (Turtle Ck), landfill leachate collection system (Harrington's Quarry) and from a sampling point penetrating a former trench (located at a collapse site, see Payne et al., 2013).

Background groundwater samples were collected from selected monitoring wells in the Kulnura-Mangrove Mountain Aquifer (KMMA), excluding shallow groundwater near agricultural developments. Monitoring wells in the KMMA are screened within Hawkesbury sandstone with several shale horizons intersected during well construction (Cendón et al., 2014). The KMMA has several groundwater bottling plants and no pollution sources were identified in the selected samples.

Groundwater samples were collected following the methods detailed in Cendón et al. (2014, 2015). Once wells were purged, pumped water was filtered in-line (0.45 μm) and directly collected into preconditioned HDPE 250 ml bottles and acidified with double distilled ~70% HNO_3. The water samples include dissolved and colloidal fractions (<0.45 μm) and therefore represent mobilised REY, in line to the approach utilised by other authors (Leybourne and Johannesson, 2008). Lawrence et al. (2006) found minimal differential effects between 0.22 μm and 0.45 μm filtration and concluded that filtration alone does not induce anomalous REY behaviour. To test the applicability of this finding in our current study, several samples were collected in duplicate and filtered through a 0.22 μm membrane (Table 1 Supplementary). Concentrations in the 0.22 μm samples were similar to those in the 0.45 μm counterparts and more importantly the differing filtration did not affect the normalised REY distribution patterns.

The REY in water samples were analysed by automated chelation preconcentration (SeaFast, ESI) followed by ICP-MS determination. Samples are automatically loaded onto a loop and injected to an iminodiacetate column that chelates all REY but allows matrix elements such as Na^+, Cl^-, Ca^{2+}, Mg^{2+} and more importantly Ba^{2+} ions to be rinsed out. The preconcentration set-up used allows a ~20-fold pre-concentration, reducing matrix interferences particularly polyatomic interferences (BaO and BaOH) on key REEs (Dulski, 1994). All mobile phases (ultra-pure >18.2 $M\Omega\ cm^{-1}$ water, acetate buffer and 2% HNO_3) are also treated by scrubber columns, therefore improving blank levels and detection limits across all REY. After pre-concentration, elements of interest are eluted with a 2% HNO_3 solution containing an internal standard (1 ppb In) and detected by a ICP-MS instrument (Varian 840). Samples, calibration solutions and external standards followed the same pre-concentration process. The isotopes selected for analysis were ^{89}Y, ^{139}La, ^{140}Ce, ^{141}Pr, ^{146}Nd, ^{147}Sm, ^{153}Eu, ^{154}Gd, ^{156}Gd, ^{157}Gd, ^{159}Tb, ^{163}Dy, ^{165}Ho, ^{166}Er, ^{169}Tm, ^{172}Yb and ^{175}Lu. Production of oxides was monitored with three solutions, each combining 1 ppb of several REE (Ce, Dy, Tb), (Nd, Sm, Gd) and (Pr, Eu) respectively. Oxide contribution to different masses was calculated with raw counts corrected for each independent analytical run. Efficacy of Ba removal was also monitored in all analytical runs with a Ba solution.

Precisions were checked with the analysis of external standards SLRS-4 and 5, a standard river water reference material for trace elements (Table 2 Supplementary). While SLRS-4 and 5 river water do not have REY certified concentrations, results have been amply reported in the literature, providing an effective tool to check analytical precision (Lawrence and Kamber, 2007; Bayon et al., 2011; Iwashita et al., 2011; Rousseau et al., 2013; Yeghicheyan et al., 2013 amongst many others).

Tritium (^3H) in LFLS groundwater constitutes a good source tracer and can be compared with REY interpretations. ^3H has been historically analysed at the site and has concentrations several orders of magnitude above natural background. Samples were collected simultaneously with REY samples and pre-concentrated using the Eichrom sample preparation technique followed by liquid scintillation analysis as reported in Hughes et al. (2011).

Solid samples from LFLS (W2D, BHF and LH-2) and other locations in the region, intersecting the same geological units (GW271007 and GW271012), were analysed for REE. Samples from W2D and regional KMMA monitoring wells were drill chips, recovered during well construction in 2010 and 2008 respectively. Samples from BHF and LH-2 came from cores drilled in 1984 by the Department of Mineral Resources New South Wales (NSW) and subsampled for this study at the NSW Drillcore Library. Solid samples from LFLS represent sites directly upgradient from trenches (W2D) and downgradient from trenches (BHF, LH-2). Due to the nature of the samples, two different analytical techniques were employed.

Drill chips were analysed by neutron activation analysis (NAA) for suitable REEs (except Er and Y). The multi-elemental NAA was carried out using the OPAL research reactor (Bennett, 2008). NAA samples were crushed and homogenised with two 50–80 mg subsamples taken to facilitate both short and long-nuclide NAA analysis. One set of subsamples were irradiated for 30 s at a neutron (n) flux of 2×10^{13} $n/(cm^2 s)$ and gamma-ray spectra taken 18 min after irradiation to detect elements which produce short-lived neutron activation products, including Dy. The remaining elements were analysed by irradiating the second subsample for 5 h at a neutron flux of 4.5×10^{12} $n/(cm^2 s)$. Gamma-ray spectra were taken 4 and 14 days after irradiation. The k_0 method of standardisation was applied using dilute gold wires for standards. The Windows software package Kayzero was used for calculation of elemental concentrations. Detection limits were calculated from measured spectral backgrounds using the method of Currie (1968) and generally ranged from ppb or ng/g (eg.: Sc, REEs) to ppm or mg kg^{-1} (eg.: Fe). Detection limits varied according to the different elements from 0.01 mg kg^{-1} in the case of Eu to 9.3 mg kg^{-1} for Pr. Most analysed REE approximated ~0.4 mg kg^{-1}, except Er and Y are at ppm or %-weight range respectively and could not be analysed because their spectra occur in the same range as hundreds of short-lived activation products. REEs results are provided in Table 3 (Supplementary).

Core portions were analysed with a non-destructive technique to preserve subsamples for textural analysis. Additionally, drill chips from W2D at LFLS were also analysed for comparison. Elemental distributions were assessed using X-ray fluorescence (XRF) in an ITRAX core scanner

(Croudace et al., 2006). ITRAX provides high resolution (<1 mm) count measurements of selected elements along analysed core portions. However, we did not use this technique quantitatively, as most REY had very low count numbers. Hence, only selected elemental count trends for Fe, Nd and Gd are reported (Table 4, Supplementary).

REY anomalies can be quantified, providing a tool to investigate elemental variations. In order to do this we normalise REY concentrations and calculate anomalies (REE/REE_N) using weighted neighbours, expressed as Sm/Sm*, Eu/Eu* and Gd/Gd* respectively. We follow the equation scheme in Olivarez and Owen (1991) (e.g.: Eq. (1)).

$$Eu/Eu* = \log 10[(Eu/Eu_{PAAS})/(2/3(Sm/Sm_{PAAS}) + 1/3(Tb/Tb_{PAAS}))] \quad (1)$$

where Eu/Eu_{PAAS}, Sm/Sm_{PAAS}, and Tb/Tb_{PAAS} are the Sm, Eu and Tb concentration in groundwater divided by the Sm, Eu and Tb concentration in PAAS respectively. In the case of Sm/Sm* and Gd/Gd*, elemental anomalies are calculated using immediate REY neighbours, while in the case of Eu/Eu* we compare to Tb (Eq. (1)), as Gd is generally associated with similar anomalies in Eu. Non-natural isotopic ratios of stable Nd, Sm, Gd, or other multi-isotopic REY elements could potentially differentiate specific anthropogenic sources (e.g.: Isnard et al., 2005), however, these were not assessed in our samples.

4. Results

REY concentrations in groundwater and REE in solids have been analysed in a total of 189 samples (Table 1, Supplementary). In the case of groundwater, monitoring wells were sampled across multiple years. Groundwater physico-chemical parameters varied depending on interacting lithologies, waste or preceding climatic conditions. In general, samples near trenches had low TDS (~200 mg L^{-1}) increasing in depth to the shale and sandstone (~3500 mg L^{-1}). Most groundwater samples were acidic and of the NaCl type. Details can be found in Table 1 (Supplementary) and Cendón et al. (2014, 2015) for regional and LFLS data respectively.

4.1. Groundwater

Kulnura-Mangrove Mountain Aquifer (KMMA) regional groundwater samples show a large range of total REY summed concentrations (ΣREY) ranging from 0.023 to 2.1 μg kg^{-1} (Table 1 Supplementary, Fig. 2). In general, normalised patterns are quite flat, i.e. maintain typical PAAS ratios (Fig. 3-A), except for small Eu depletions that may result from weathering of local basaltic diatremes. These samples are considered representative for groundwater obtained from the Hawkesbury sandstone and are used to assess REY background behaviour. Groundwater samples at the LFLS site have a wide range of ΣREY, with P1S (down-flow from the trenches) showing the highest sum of concentrations averaging 237 μg kg^{-1} (Table 1 Supplementary). The lowest ΣREY were in samples farther from the trenches and close to Harrington's Quarry, particularly in shallow wells W2S and W2M with the sum of REY concentrations averaging 0.11 μg kg^{-1}. Overall LFLS samples had an average ΣREY concentration of 31 μg kg^{-1}, compared to 0.43 μg kg^{-1} observed in regional background sites. Yttrium represents an elevated proportion of the overall ΣREY concentrations. There is an increase in the proportion of Y with depth. In samples near trenches Y represents an average 11% of the total ΣREY, while for groundwater monitoring wells screened within shale and sandstone, yttrium represented 34% and 54% of the ΣREY respectively.

Leachate samples were collected directly from the landfill leachate collection system and a monitoring well adjacent to Harrington's Quarry landfill (Fig. 1, Table 1 Supplementary). Physico-chemical parameters were measured in one sample showing high TDS (7838 mg L^{-1}), a pH of 6.97, an Eh of 78 mV and a high alkalinity of 2660 mg L^{-1} $CaCO_3$. The ΣREY varied from 0.1 to 0.6 μg kg^{-1} and were lower than in groundwater samples. REY analysis of digested solid landfill-waste from four waste sites in the UK averaged 53 mg kg^{-1} (Gutiérrez-Gutiérrez et al., 2015), with PAAS-normalised patterns relatively flat, compared to those obtained from the landfill leachate in our samples.

Fig. 2 shows the relative differences between groups of REEs according to location and sample interactions. Shallow monitoring wells around the waste trenches form a group characterised by high concentrations of MREE, sitting above regional background samples. Older wells (i.e. "long-

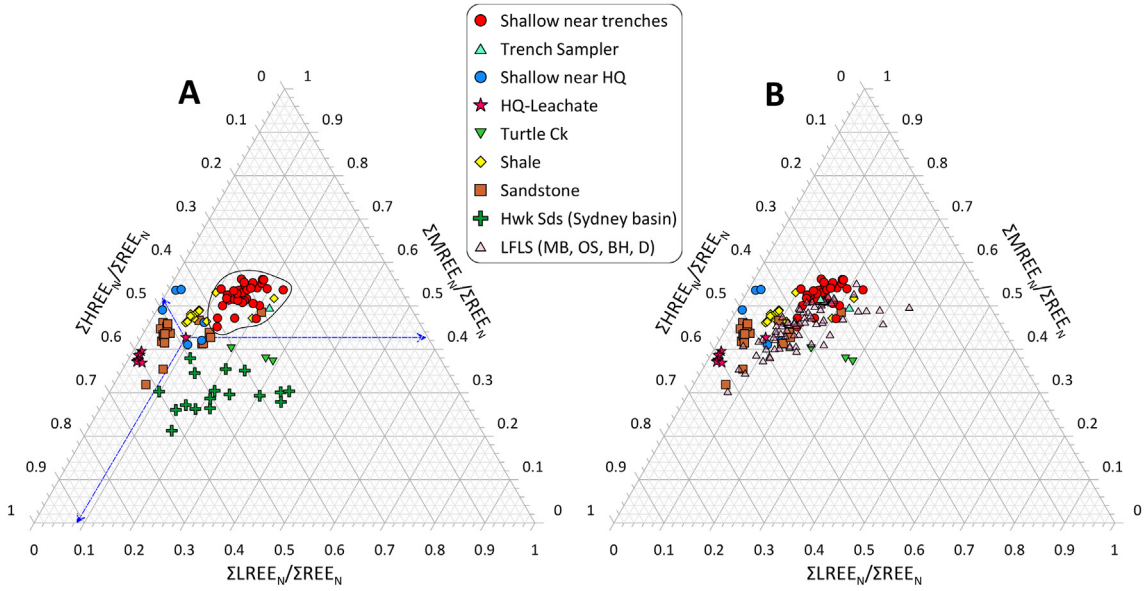

Fig. 2. Tri plots showing the sum of PAAS normalised concentrations for LREE (La to Nd), MREE (Sm to Dy) and HREE (Ho to Lu) divided by the sum of REEs normalised concentration for each sample. Yttrium is excluded in these plots so that REEs variations can be better appreciated. Concentrations are normalised to removed biases due to differences in elemental abundance. Wells screened near trenches, shale and sandstone are differentiated, as well as samples obtained from the leachate system, Turtle Ck pools and trench sampler. A) Groundwater samples from screened monitoring wells only. Samples from the trench area are circled for reference. Values of groundwater in Hawkesbury Sandstones from the Kulnura-Mangrove Mountain Aquifer (dark green crosses) are included for reference. The blue arrows show how to read the axes; B) Complete LFLS dataset including groundwater samples from older monitoring wells, not differentiated due to long-screens and potential mixing. Details for these older MB, OS, BH and D wells can be seen in Cendón et al. (2015).

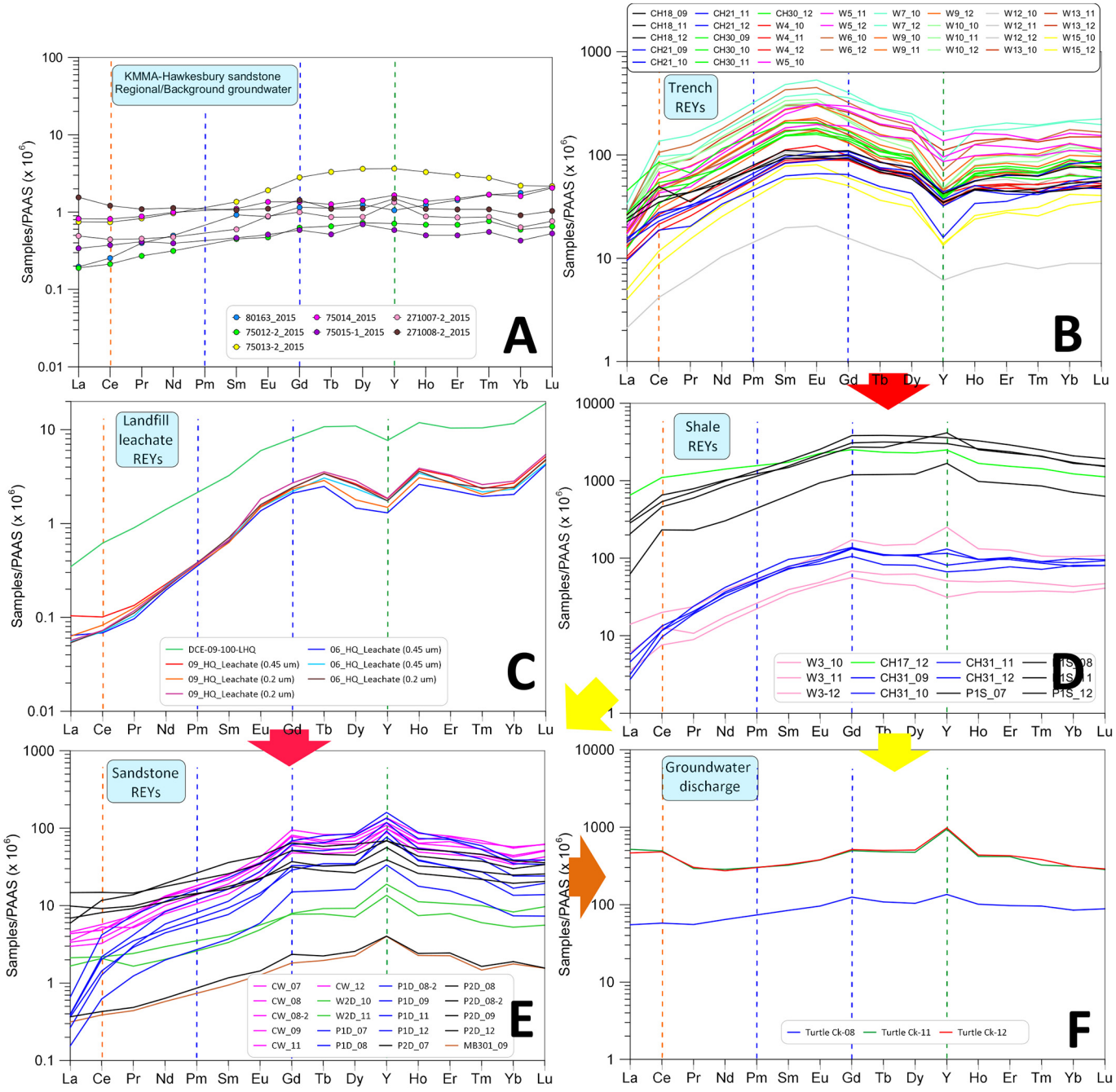

Fig. 3. PAAS normalised patterns for LFLS water samples grouped by sample. Available sampled years are indicated in legend. A) Background groundwater samples in the Sydney Basin obtained from the KMMA. (Fig. 1); B) Samples around LFLS waste trenches; C) Groundwater from the leachate collection system; D) Groundwater samples from wells screened within the weathered-fresh shale transition; and E) Groundwater samples screened in the underlying sandstone. F) Groundwater discharge sampled from seeps in Turtle Ck. Vertical dotted lines merely assist identification of elements. Arrows are depicted to indicate groundwater movement at the Little Forest site. Arrow colour scheme follows that of Fig. 2.

screen") show greater scatter with samples showing a potential degree of mixing (Fig. 2-B). Groundwater recovered from deeper monitoring wells, either in the transition between shallow weathered-fresh shale or deeper in sandstone, shows a considerable depletion in LREEs and plot to the left, with relative enrichments dominated by HREEs. Samples from landfill leachate also show a relative abundance of HREEs.

In general, REY groundwater concentrations can vary greatly, exhibiting seasonal dilution or concentration via evapotranspiration. The PAAS-normalised trends better preserve the fingerprint of REY for each groundwater sample, while relative concentrations can still be assessed on the Y-axis (Fig. 3). Patterns in general are quite consistent at specific sites for all yearly samples, with some sites sampled annually over six years (e.g. CW).

Groundwater samples within the trenched area (Fig. 3-B) show occasional Ce enrichments in shale-normalised patterns with respect to near neighbours. MREEs show a marked enrichment in samarium, europium and gadolinium. Yttrium, on the other hand, appears systematically depleted near trench areas. Monitoring wells screened in the weathered/fresh shale transition (Fig. 3-D) show groundwater that preserves a Ce enrichment while Gd appears increasingly enriched amongst MREEs. Yttrium

in these samples shows similar, but variable enrichment. Deeper groundwater samples obtained in the shale and/or the sandstone are variable in Ce, while a systematic enrichment in yttrium and gadolinium is observed. The deepest sample (P2D) shows a tendency for LREEs to be less depleted with flatter REY patterns regardless of the year sampled, closer to results observed in regional groundwater. Shallower P1D and CW show middle and high REE enrichments compared to P2D. All P1D, P2D and CW show a Y enrichment (Fig. 3-D).

Samples of groundwater discharge collected from a pool along the Turtle Creek in three different years (Fig. 3-F), show a consistent pattern, which resembles P2D or sandstone samples. Fig. 3 shows the potential groundwater flow directions between groups (arrows) and therefore the direction of groundwater evolution following recharge at the site.

Samples from the landfill leachate (Fig. 3-C) show a complex pattern with MREE enrichments in Eu, Gd reaching a maximum in Tb and then HREE enrichments in holmium and lutetium. All leachate samples appear depleted in Y while the MB301 sample collected in the proximity of Harrington's Quarry shows an enriched yttrium like the sandstone and some shale samples. Tritium results in groundwaters from short-screened monitoring wells sampled between 2007 and 2009 were reported in Hughes et al. (2011) and Cendón et al. (2015). Samples from 2010 to 2012 comprising a total of 64 analysis are reported in Table 1, Supplementary. In general, tritium activities ranged from 10,860 Bq L^{-1} (~92,033 TU) between trenches at monitoring well W10 (2010) to 0.92 Bq L^{-1} (~7 TU) in P2D (2012), a deep well at the site screened in the underlying sandstone.

In summary, the REE data obtained for groundwater in this study clearly differentiates the different water types both in terms of relative concentrations, visualised by sample position in the tri-linear plots (Fig. 2), as well as the shapes of normalised REE patterns (Fig. 3).

4.2. Drill chips and core samples

Concentrations of the lighter LREE in solid LFLS samples are generally higher than the rest of REE, for example Ce has a concentration of 131 mg kg^{-1} in sample W2D (4.5–5 m). Minimum concentrations are found for HREE, particularly Tm, for example sample GW271007 (4–5 m) with 0.12 mg kg^{-1}. This reflects general elemental crustal abundance for REY.

Normalised patterns in solid samples at LFLS appear relatively flat with values close to unity, except for shallow samples. These flat profiles results from the standardisation with PAAS (shale), indicating that samples from LFLS have REY distributions similar to shale. The exception to the general trend of flat REY patterns is Lu, which exhibits enrichment (Fig. 2, Supplementary). This enrichment could be an analytical artefact in the NAA affecting all samples similarly, irrespective of origin. While NAA analysis of reference material (NIST 2711a Montana II Soil) showed similar results to those reported elsewhere, concentrations for Lu are not certified and its neutron activation behaviour deviates from the simpler neutron activation models, requiring additional corrections.

In the case of regional solid samples recovered from the geological materials at GW271007 and GW271012, the samples from intervals 4–5 m and 47–48 m were depleted in all REE, compared to PAAS. In the case of shallow samples this could be related to leaching of REEs from the topsoil profile of the local Podzols, as documented in similar soils elsewhere (Vermeire et al., 2016). Depletions in deeper samples (47–48 m) could be related to lower clay contents, fluctuations in groundwater levels or increased groundwater flow within those intervals favouring leaching. In general, NAA results upstream of trenches do not show REE enrichment with respect to crustal abundances, with similar flat REEs trends in regional samples from the same geological materials.

X-ray counts (ITRAX) for Fe, Gd and Nd are higher in the shallow weathered materials with a strong correlation between Fe and REEs (Fig. 2 and Table 4 supplementary). Count peaks coincide with fractures or partings in the sediments where iron hydroxide minerals FeOOHs have precipitated and are visible in core samples.

5. Discussion

REY behaviour during water-rock (and/or waste) interaction is controlled by solution complexation and adsorption (Tang and Johannesson, 2006; Liu et al., 2017). The two principal REY complexing (and mobilising) agents at Earth's surface are dissolved organic matter (DOM) and carbonate ions (Tang and Johannesson, 2006; Pourret et al., 2007), while adsorption takes place onto pre-existing FeMn oxyhydroxides and particulate organic matter (POM) surfaces (Liu et al., 2017). The efficiency of complexing and adsorption processes is affected by physico-chemical conditions (i.e. pH, REDOX) (Dinali et al., 2019) with additional controls occurring during co-precipitation with iron hydroxide minerals (FeOOH) (Bau, 1999).

Current research highlights pH as a key controlling factor for sorption, with solution sorbate concentration potentially playing a secondary role (Tang and Johannesson, 2010). Recent laboratory experiments (Liu et al., 2017) have demonstrated sharp variations in REY sorption onto FeOOH resulting from small pH variations. Generally, at low pH (<5) the sorption is low (<10%) while a sharp increase takes places at circum-neutral pH to reach a maximum (>90%) at pH ~8 for all REEs. This behaviour is first noticed around pH ~ 5 for HREE and then propagates to MREE and LREE respectively as pH increases towards 8.

In the case of dissolved organic matter, laboratory experiments show that the presence of DOM enhances sorption of REE to sandy sediment, with slight variations depending on organic matter nature (fulvic vs humic acids) (Tang and Johannesson, 2010). Maximum REE sorption takes place at pH ~ 4 (60–80% sorption) reducing with increasing pH with a similar preference for HREE first, followed by MREE and LREE. However, laboratory experiments seem to contrast with field scale observations. Tracer experiments at the Oak Ridge disposal site (USA) showed the almost simultaneous arrival of injected Nd and Eu and the conservative tracer (Br^-) to the control well (McCarthy et al., 1998a, 1998b). The same authors proposed that DOM-REE complexes formed in the groundwater, enhancing transport of REY and therefore transuranic elements. The abundance of anthropogenic organic matter in the co-disposed waste (i.e. Rowling et al., 2017), leads to a complex series of interactions, including competition for sorption sites in the aquifer matrix, as well as solution phase complexation. This latter interaction may involve the formation of organic REEs complexes which may mobilise downgradient, particularly after large storms.

The following discussion follows the processes highlighted above on a natural scale. The density of sampling points at LFLS allow for groundwater REY distributions to be assessed at different depths and processes inferred. The REY distributions in groundwater can be compared to those in the aquifer host materials, both locally and regionally, differentiating local processes and increasing our understanding of REY in contaminated sites. Considering the highly instrumented nature of many landfills and other waste facilities globally the workflow presented has a wide potential application.

5.1. Fingerprinting REY sources and distributions at LFLS

Four types of waste storage areas are present in the vicinity of LFLS (Fig. 1) and they provide potentially different pollutants at the Little Forest site: a) low level legacy waste "LFLS trenches"; b) municipal solid waste landfill located in the unlined pit of the former Harrington's Quarry; c) industrial liquid waste disposal (IWC) and d) household organic waste from pit latrines "night soils". The distribution of groundwater monitoring wells is concentrated within the LFLS and neighbouring Harrington's Quarry. Potential contributions from the night soils area are unlikely as they are downgradient of LFLS, however, they were not accessible to be assessed. The shale extractions, prior to landfill (Harrington's Quarry), modified the original geology. In general, three geological domains can be distinguished at Little Forest under the LFLS trenches: topsoil/weathered shale, shale and sandstone. These are reduced to one (sandstone) in the Harrington's Quarry and IWC areas due to the mining of the shale. Fig. 4 provides a cross section to aid the conceptualisation of the area with

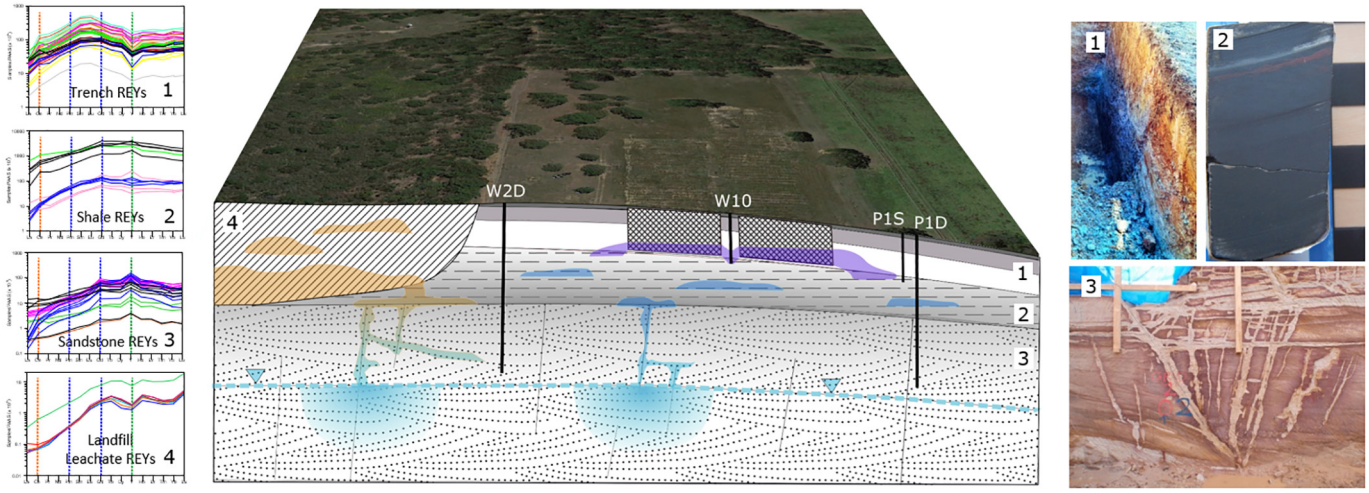

Fig. 4. Block diagram of the LFLS. The extension of the trenches is outlined for reference. 1) Trench excavated at the LFLS showing undisturbed soil and weathered shale; 2) Shale obtained from core BHF sample DCE-16-67 (870-875 cm) (Supplementary Fig. 2); 3) Hawkesbury sandstone section during digging of foundations ~1.8 km south of LFLS. REY normalised trends in groundwater (1, 2, 3, 4) are linked to their respective waste and/or geological context.

discussion generally referring to two potential pollution sources (Trenches and Landfill/IWC) and three-layered geological materials when discussing the LFLS trenches.

5.1.1. LFLS trenches

The ΣREY concentrations in shallow groundwaters near trenches are relatively high, with a median of 11.5 μg kg^{-1}, compared to 0.27 μg kg^{-1} for samples in other non-polluted locations of the Sydney Basin. However, concentrations can vary greatly, exhibiting seasonal dilution or evapotranspiration. The median pH for groundwater sampled around trenches is 4.3 (±0.6) with very low alkalinity. Dissolved organic carbon concentrations show large variations (Cendón et al., 2015). For example, well MB16, located close to W10, had a DOC concentration of 48.4 mg L^{-1} in August 2007, soon after a large rainfall event in June 2007 that followed 7 years of below average rainfall, compared to 0.68 mg L^{-1} in March 2008 after months above average rainfall.

MREE elements are used in the nuclear industry, due to their high neutron cross-section capture, which makes them useful for shielding, moderation or shutdown of reactivity (Ray, 1971; Bourg and Poinssot, 2017). Apart from waste that is derived from reactor research (Payne et al., 2020), other sources of MREEs at LFLS would include production of radiopharmaceuticals and experimentation on the neutron capture cross-section of Sm (Whittem, 1968). Near the waste trenches, groundwater shows consistent REY patterns with MREE enrichments (especially Sm, Eu and Gd), which are not affected by seasonal variations (Fig. 3-B). On the other hand, regional groundwater shows relatively flat REY patterns (Fig. 3-A). Distributions of REE in rocks from LFLS and regionally show flat trends with ratios close to unity (Fig. 2, Supplementary) as those reported for the upper crust elsewhere (PAAS). These direct comparisons exclude natural MREE enrichment in the aquifer matrix materials.

Large rain events cause the underlying shale-lens waste trenches to be waterlogged, forming “bathtubs” where water accumulates and interacts with waste (Payne et al., 2013). Therefore, the observed REY enrichments in groundwater near trenches can be explained by water-waste interaction (Fig. 3-B). This point is reinforced by the physical setting and observed high tritium activities in co-sampled groundwater (Hughes et al., 2011), the presence of actinides (Payne et al., 2020), high iodide concentrations and very low Cl/Br ratios (Cendón et al., 2015), which are all associated with trench-waste-groundwater interaction. In summary, the distinctive MREE enriched patterns near trenches reflect REY waste-groundwater interactions in the trench prior to recharge into the regional groundwater in the underlying sandstone. The low pH allows REY to remain in solution and minimises sorption onto FeOOH, while the seasonally high DOC concentrations may enhance the formation of REY-DOC complexes.

5.1.2. Landfill and/or industrial leachate

Adjacent to the LFLS, percolating rainfall interacts with household municipal landfill waste (Harrington's Quarry) and other liquid industrial waste disposal pollution sources (Cendón et al., 2015). Recharge pathways laterally or vertically down-gradient towards the regional groundwater level vary greatly, according to the presence or absence of shale, fractures and potential cones of depression generated by pumping and processing of leachate.

Several leachate samples were directly recovered from the leachate collection system at Harrington's Quarry. The leachate has a circumneutral pH, low Eh, high total dissolved solids (TDS) and high alkalinity. This contrasts with the generally acidic, low alkalinity, low TDS and well-oxidised groundwater intercepted around LFLS trenches. Leachate REY patterns are quite consistent, regardless of filtration pore size (0.22 or 0.45 μm) and different to those near trenches or anywhere in regional non-polluted groundwater. Leachate is characterised by depleted LREEs with an increasing enrichment trend and a maximum in Tb, Ho and Lu (Fig. 3-C). Johannesson et al. (1997) argued that the formation of strong REE carbonate ion complexes in solution, particularly with the HREEs, can enhance their effective solubility. However, the strong pH gradient towards more acidic groundwater in depth away from the leachate would make REY-carbonate complexes unstable. The strong REDOX gradient also potentially favours precipitation of FeOOHs. In summary, the REY contributions from the landfill, while lower in total concentration, are not impeded by (quarried-out) confining layers. The strong chemical gradients away from the leachate modify REY patterns in very close proximity to Harrington's Quarry, with REY trends evolving towards those found in the surrounding sandstone (i.e. MB301).

5.1.3. Shale and sandstone

Below the trenches, the presence of dry horizons intersected during drilling demonstrates the perched nature of shallower groundwater near trenches. Therefore, there is a gradient downwards to the regional groundwater level ~ 12 m below surface in the underlying sandstones, with vertical flow hindered by the intervening shales (Hughes et al., 2011). The groundwater in shales has a low pH (4.1 ± 0.8) and relatively high TDS compared to groundwater in the trenches above or the underlying sandstone. Shale groundwater samples at LFLS show variations in normalised REY patterns with depth compared to groundwater near trenches (Fig. 3 CD). Two closely located monitoring wells (CH30 and CH31) illustrate

the transition between groundwater near trenches and shale. Groundwater at CH30, screened close to the base of the trenches, has trench-like patterns while CH31 screened 3–4 m below trenches shows that MREE anomalies are generally smoothed out, excepting Gd and Y discussed below (Fig. 3 BD). The reduced hydraulic conductivity of the shales and additionally the low ^{3}H activity found in groundwater samples recovered from shale-screened monitoring wells suggest limited downward groundwater flow. In summary, the low pH below the range of bicarbonate ion stability, favours DOC-REY complexes as a transport mechanism in the trench-shale transition areas. The groundwater level fluctuations and redox variations favour precipitation of FeOOHs, particularly along fractures as can be seen in core samples from BHF (Fig. 1 Supplementary). Detailed ITRAX analysis further supports REEs associated with the FeOOHs in the fractures (Fig. 2 Supplementary).

Below the regional water table, in the sandstone, REY patterns are similar to those in the shale with higher Gd and Y positive anomalies and potentially other subtle variations in HREE. Hydrochemical conditions of groundwater with depth shift to a higher pH (5.4 ± 0.3), as some of the acidity is neutralised by dispersed carbonates in the sandstone (Cendón et al., 2014). The Gd anomaly is totally absent in regional groundwater samples, while two regional samples (271007-2 and 271008-2) show a positive Y anomaly (Fig. 3-A). Overall regional groundwater samples show very different REY trends to those observed at LFLS, despite being collected from materials of the same age and lithologies. In summary, REY trends observed in deeper sandstone groundwater show the effect of anthropogenic inputs particularly on Gd. Precipitation of FeOOHs and the slightly higher pH favours preferential sorption of other REY onto FeOOHs compared to Gd and Y.

5.2. Evolution of REY anomalies at LFLS

Groundwater REY trends in natural settings, while related to water-rock interactions in the aquifer matrix, are not necessarily like those observed in the aquifer parent rocks (Fig. 2 Supplementary) (Möller et al., 2006; Leybourne and Johannesson, 2008). This difference is driven by physicochemical interactions between groundwater and surrounding materials and the slightly different interelement solubility behaviour of REY. As discussed above, two type of anomalies are evident at LFLS: MREEs enrichment, particularly Gd, and the sharp departures of Y.

5.2.1. MREE enrichments

Calculated anomalies, displayed in Fig. 5, differentiate groups of samples according to nearest waste source, geological materials, depth and processes. Regional (KMAA) groundwater samples show very low enrichments

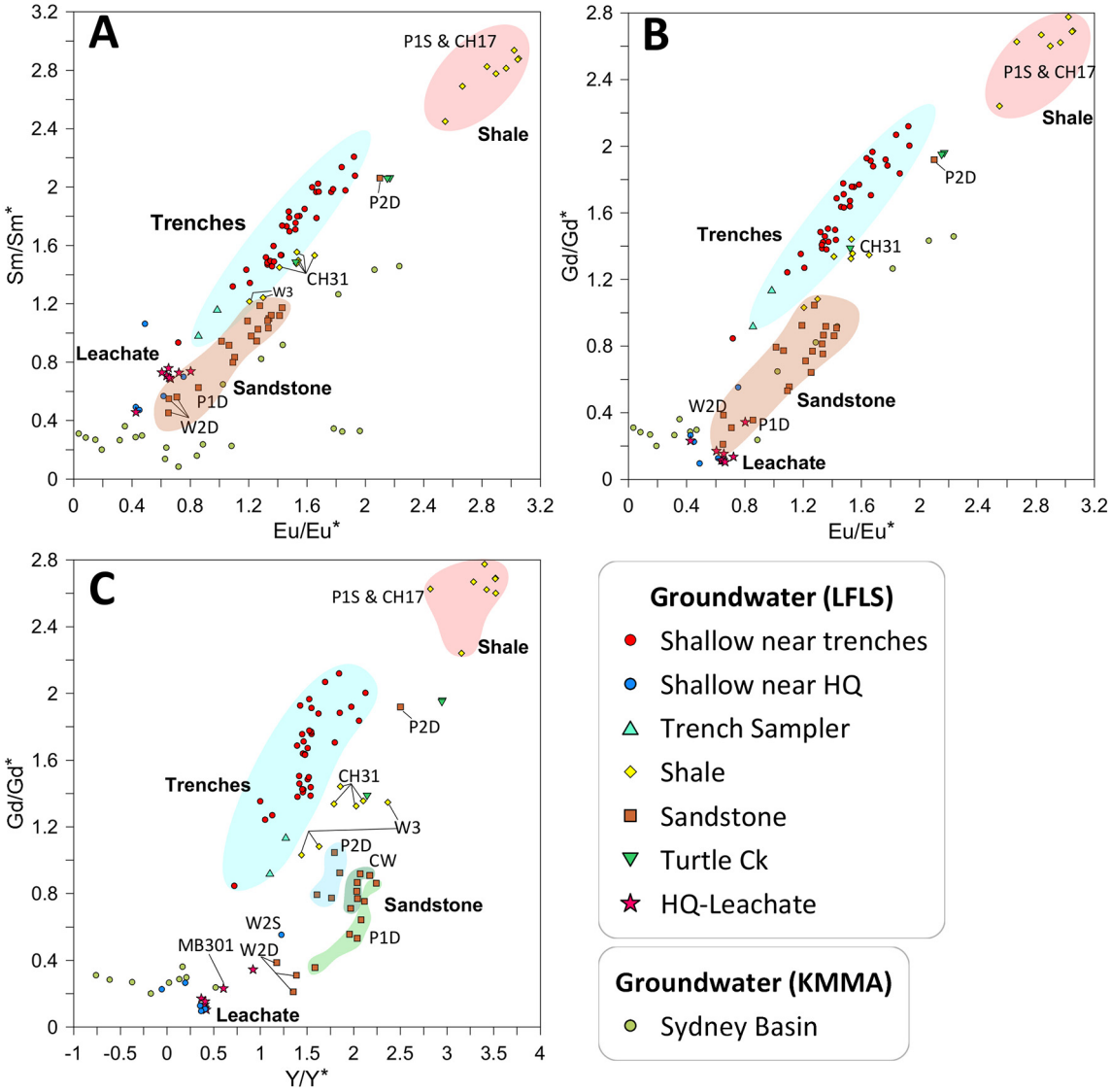

Fig. 5. A) and B) Calculated anomaly ratios of Sm/Sm∗ and Gd/Gd∗ against Eu/Eu∗ ratios. C) anomaly ratios of Gd/Gd* against Y/Y*. Some samples are labelled for reference; their locations can be seen in Fig. 1. Anomalies from KMMA groundwaters are also displayed for reference.

in MREE or even depletions in the case of Y/Y*. Groundwater near trenches shows enrichments in all MREE and define a relatively homogeneous group. In the shale groundwater samples exhibit two different types of anomalies: a) groundwater samples with high anomalies in all MREE (~3) (P1S and CH17); and b) groundwater samples with lower anomalies (~1.6) (CH31 and W3). The two monitoring wells in the first group are situated at opposite sides of LFLS, away from the trenches, while the second group is close or directly under trenches (Fig. 1-C). The large, non-natural, MREE anomaly detected at P1S and CH17, suggest REY transport away from trenches has taken place since LFLS closure. Whether the lower REY anomalies detected in groundwater under trenches at the present time, compared to distant monitoring wells, suggests attenuation of anomalies through time or specific pulse conditions, cannot be assessed.

Shallow groundwater near HQ landfill shows MREE anomalies like those in HQ leachate samples (e.g. W2S, W2M, MB301). As depth increases, groundwater in the sandstone shows trends suggesting different seasonal contributions or mixing. For example, sample P2D, obtained in 2007 after the long drought in eastern Australia, shows enrichments characteristic of LFLS trench signatures. However, after above average wet periods in the rest of samples to 2012, all enrichments decreased to values closer to those found in the HQ leachate. The absence of shale below the landfill allows a direct pathway for contaminants, with above average rainfalls potentially overwhelming the leachate-capture system at times. This would facilitate down-gradient recharge and the enrichment signatures observed.

MREEs anomalies particularly for Sm and Eu decrease with depth due to REY scavenging and/or sorption on to precipitated FeOOH. In contrast, a Gadolinium enrichment in shale-normalised patterns is observed with respect to its near neighbours. Its presence may be linked to household/industrial waste (i.e.: old cathode tubes, metallurgy). Positive Gd anomalies are well documented in urban streamflow settings, particularly related to sewage treatment plants and waste inputs from modern medical procedures (Möller et al., 2002; Knappe et al., 2005; Rogowska et al., 2018).

5.2.2. Y/Ho ratio enrichments and depletions

The other noticeable anomaly detected in the Little Forest area affects yttrium (Fig. 3 and 6C). Yttrium and Holmium generally behave equally, due to their similarity in ionic radii and charge. Both elements exhibit quite constant ratios (Y/Ho) in igneous rocks and clastic sediments (mass ratio, $Y/Ho_{(PAAS)}$ = 24–34). However, Y/Ho in groundwater generally departs from the ratio found in solids (Tweed et al., 2006). This is also observed in the Sydney Basin regional groundwater samples that have Y/Ho ratios ranging from 24 to 57 with an average of 37 (n = 18) with some noticeable Y enrichments in PAAS normalised trends (Fig. 3-A). The difference in Y/Ho groundwater ratios arise from the slightly different behaviour of Y and Ho in solution and the role of FeOOHs in controlling Y and scavenging of REEs, discussed below. Dissolution/precipitation of FeOOHs is ubiquitous in the regional geology (Wray, 1995; Cendón et al., 2014) potentially enhanced by bacterial mediated reactions (Heim et al., 2015). Iron concentrations in groundwater at the LFLS increase with depth as REDOX conditions favour its presence as soluble Fe^{2+} (Table 1, Supplementary). Conversely, Fe concentrations in sediments increase in the top 5 m, with oxidative conditions favouring precipitation. NAA analysis of sediments from W2D show high iron concentrations, increasing in the top 5 m up to 176 g/kg. Similarly, ITRAX count rates for Fe are much higher in materials close to surface showing strong correlation with REEs (Fig. 2, Supplementary).

The distribution of Y/Ho ratios in LFLS groundwater clusters samples into three groups associated with their respective sources/interactions: trenches, shale and sandstone (Fig. 6-A). Groundwater Y/Ho ratios at LFLS range from 11 to 66, displaying a tri-modal distribution, with ratios around 17, 33 and 46 (Fig. 6).

As demonstrated by Bau (1999) and Kawabe et al. (1999), Y has a different behaviour to REE, particularly during precipitation of Fe-oxyhydroxide (FeOOH). Y has also a lower affinity for Fe-oxyhydroxides than Ho, so scavenging of dissolved REY during FeOOH precipitation will modify REY in solution, with Y enriched in groundwater. This process would also result in positive anomalies in shale normalised patterns of the non-redox-sensitive elements La, Gd, Y and possibly Lu (Fig. 3). All these positive anomalies are observed in deeper (sandstone) groundwater samples at LFLS, except for that of La in some samples (Fig. 3-E). Interestingly, all trench groundwater samples have negative Y anomalies with respect to surrounding REEs. This is consistent with a lower Y input during water-rock-waste interaction, while other expected anomalies (La, Lu) are not observed or are masked by high MREE concentrations (Gd). Whether the waste is currently Y-impoverished, or Y has been preferentially mobilised offsite over time cannot be ascertained. Additionally, interactions with trench-fill materials containing FeOOHs could also contribute to the negative anomaly near trenches. The presence of some positive Y anomalies in groundwater elsewhere in the Sydney Basin (Fig. 3-A) as well as behaviour of Y on-site (Fig. 3-E) suggest Y anomalies are overall controlled by ubiquitous FeOOH precipitation, regardless of the additional Y that may be provided

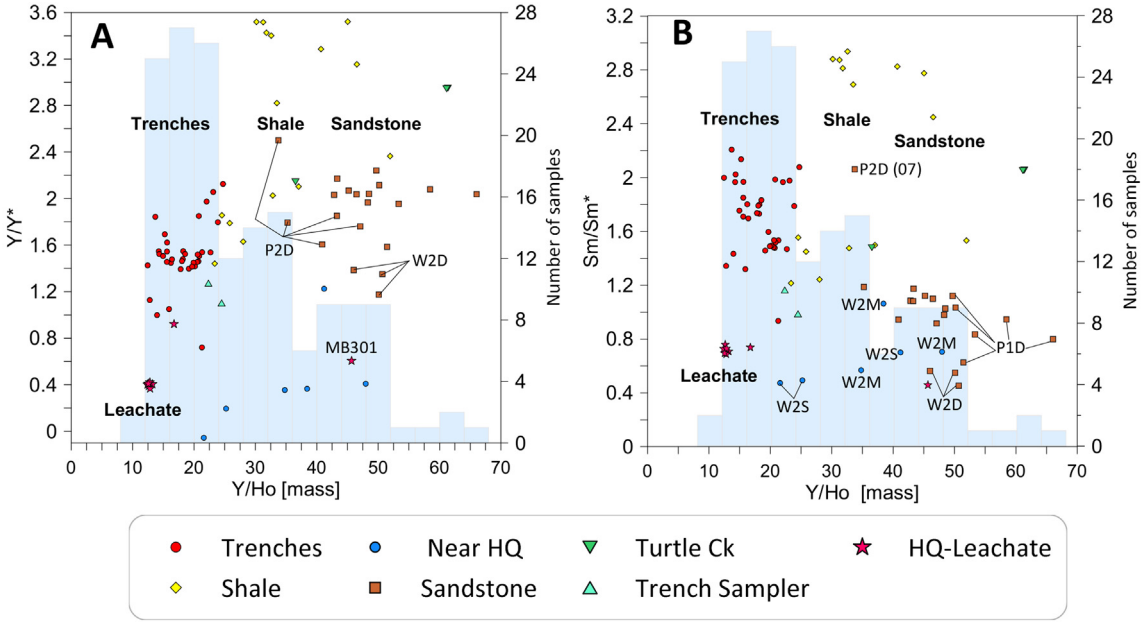

Fig. 6. A) Y/Y* values against the Y/Ho ratio in groundwater samples. B) Sm/Sm* values against Y/Ho ratio in the same samples. The blue bars (Y-right axis; number of samples) comprise a histogram of Y/Ho ratios incorporating all available groundwater ("long-screened") samples at Little Forest (Table 1, Supplementary).

by waste forms. Y increase in proportion of REY in groundwater with depth, from 11% near trenches to 54% of total REY concentration in the sandstone. This is the result of evolution along the flow path with Y favoured to remain in solution during FeOOH precipitation.

5.3. Management implications for LFLS

Limiting dispersion and mobility of contaminants is the key environmental objective at disposal sites. The US-Department of Energy controls over 30 low-level and mixed low-level disposal facilities with many other under other administrative controls in the US alone (ILLWD, 2011). The total number of legacy and operative facilities worldwide is expected to increase. The aquatic chemistry behaviour of trivalent REY is very similar to that of actinides (McCarthy et al., 1998a, 1998b; Geckeis and Rabung, 2008; Missana et al., 2008; Tang and Johannesson, 2010). While the study of actinides is outside the scope of this study, we infer that the findings derived from REY could inform trivalent actinide mobility and therefore inform management options at LFLS as well as other current and future radioactive waste disposal sites.

Generally, most detailed studies on REY/actinide behaviour focus on laboratory batch-sorption experiments under controlled conditions that do not replicate the complex combinations of conditions found in the real world; here we focus at a site scale. Two aspects affect LFLS particularly: A) the time elapsed since closure (>50 yrs) is expected to have resulted in a complex interaction of processes leading to both dispersion and natural attenuation, as observed in landfill sites (Cozzarelli et al., 2011); B) more unique to LFLS, the co-location of diverse contaminant inputs (e.g. landfill, disposal of industrial liquid wastes) makes source attribution difficult. The use of REY helps to identify the extent of contaminant dispersion and decouple processes at the site scale, informing source allocation.

Contouring the average middle REY (MREY) anomaly using Sm/Sm* in groundwater, derived exclusively from more recent screened monitoring wells around the trenches (W-series) and at similar depths, shows a NNE trend (Fig. 7). The highest Sm/Sm* anomalies around the trench area are found on the eastern margin of the trenches at W7, while the highest anomalies at the site (not captured in Fig. 7) are found within shale groundwater to the north (CH17) and south (P1S) extremes of the trench area respectively (Fig. 1). Low Sm/Sm* at W12 suggest REY subsurface movement in the south direction may be locally impeded (Fig. 7). Payne et al. (2013) demonstrated the importance of the "bathtub effect" at the site, where surface or shallow subsurface transport is a consequence of large rainfall infiltration resulting in trench filling or overflow. REY mobilisation appears subsurface to the NNE towards CH17, but as surface flow to the SSE (P1S), bypassing W12. The latter is supported by ephemeral spring flow after significant rainfall and extended waterlogged periods around P1S. The high Sm/Sm* anomalies detected at CH17 (Sm/Sm* = 2.76) (Table 1 Supplementary) compared to W7 (Sm/Sm* = 2.14) suggest the heterogeneity of the waste and that groundwater moves in pulses after large rainfall, with MREY distributions affected by mobility and/or time since burial. The similarity of Sm/Sm* at two opposite points of the trenches, with two suspected different flow mechanisms, imply that there are changes in Sm/Sm* over time, as simple dilution would not affect Sm/Sm*. No other monitoring wells tapping into the shale or sandstone are accessible downgradient of CH17 or P1S (Sm/Sm* = 2.79) but these results inform those areas are where future monitoring efforts should focus.

Sm/Sm* to the west decreases, with values consistent with mixing inputs from the neighbouring landfill at Harrington's Quarry. Values obtained from W3, screened in the shale, are also consistent with this interpretation (Sm/Sm* = 1.23). Furthermore, all REY samples from W-series monitoring wells were collected between 2010 and 2012, coinciding with a period of average to above average rainfall where discharges from Harrington's Quarry could increase. Similarly, Y/Ho ratios to the west of trenches are like those in the leachate, however, there is a sharp change in ratios with depth (W3) as discussed in 5.2.

Combining REY with ^{3}H activities in the same groundwater samples reinforces REY interpretations. The presence of ^{3}H in deeper groundwater around LFLS has been generically interpreted as linked to radioactive waste in LFLS trenches (GHD, 2003), despite elevated ^{3}H activities being well documented in landfills worldwide (Robinson and Gronow, 1996; Castañeda et al., 2012) and in local neighbouring landfills (Hughes et al., 2011). The highly elevated tritium concentrations in radioactive waste sites (such as LFLS) are associated with the disposal of highly contaminated items from nuclear operations, whereas the more moderate amounts of tritium in typical landfills arise from disposal of tritium-containing objects such as exit signs (Hughes et al., 2011). Removal of shales at landfill sites in the vicinity have enhanced the possibility of leachate seepage around the LFLS site. Moreover, groundwater ^{3}H activity levels in deeper groundwater are in general compatible with expected activities derived from landfill sources.

Shallow groundwater samples near trenches have elevated ^{3}H, particularly between the two sets of trenches around W10, with higher values also towards the NNE (Hughes et al., 2011). ^{3}H activities around trenches are up to six orders of magnitude above natural background, despite approximately four ^{3}H half-life periods since burial. MREY anomalies (e.g.: Sm/Sm*) are also high in the same NNE direction, particularly towards the eastern edge of the trench area (W7) (Figs. 7 and 8). ^{3}H in groundwater obtained from the shale shows more variability, generally decreasing with decay and distance from trenches, as groundwater mixes (dilutes) with non-polluted recharge. Despite Sm/Sm* enrichments and ^{3}H above natural background detected in shale groundwater, this unit acts as a barrier to downward transport of contaminants, as groundwater in the sandstones below generally have ^{3}H activities 4–5 order of magnitude below those near trenches and Sm/Sm* below ~1. An exception is CH31 that accesses groundwater right below the trenches (inclined well).

Fig. 8 shows that the combination of Sm/Sm* and ^{3}H captures a complex setting with mixing processes modulated by rainfall dilution and decay in the case of ^{3}H and/or seasonal pulses in the case of Sm/Sm*. Groundwater samples showing elevated Sm/Sm* anomalies and elevated ^{3}H are linked to LFLS waste near trenches while high Sm/Sm* but lower ^{3}H, farther from trenches, represent past pulses dispersing since waste burial began. In the NW corner of the site, CW shows elevated ^{3}H above those expected from landfill and relatively elevated Sm/Sm*; this monitoring well may itself be facilitating dispersion of contaminants, as it is screened close to the bottom level of trenches placing shale and sandstone in hydrological contact. The same well may play a role to explain transient elevated Sm/Sm*(2.06) identified in closely located but deeper P2D. The enrichment at P2D during 2007 followed rains that broke a continuous period of below average rainfall (Fig. 8).

Groundwater from sandstone (P1D) shows similar ^{3}H values during a six-year period (100.8 Bq L^{-1} ± 17; n = 5) (Table 1, Supplementary). P2D also follows a similar behaviour except for year 2012 that registers a 3-fold increase in ^{3}H. On the other hand, Sm/Sm* shows a parallel evolution in both monitoring wells, with decreasing values from 2007 to 2009 and increasing from 2009 to 2012 (Table 1, Supplementary). Other groundwater samples obtained from sandstones close to landfill (Harrington's Quarry) but farther away from LFLS (MB301) and upflow from trenches (W2D) show above background ^{3}H and low Sm/Sm* (Fig. 8). Considering all the above lines of evidence, seasonal variations are affecting Sm/Sm* enrichments in the sandstone groundwater. Samples are either dominated by landfill sources (MB301, W2D) or seasonal mixing between mostly landfill (P1D, P2D) and occasional pulses from trench contributions (CW). We cannot currently quantify proportions of trench derived inputs but MREE enrichment strongly suggest their seasonal presence. The current findings coupled to a site hydrological model of the site may be able to better constraint the rapid response of the system and relative contributions over time.

6. Conclusions

Groundwater monitoring networks, generally available around waste facilities like LFLS, make these highly instrumented sites the ideal setting to trace potential mobility of pollutants as well as processes along flow

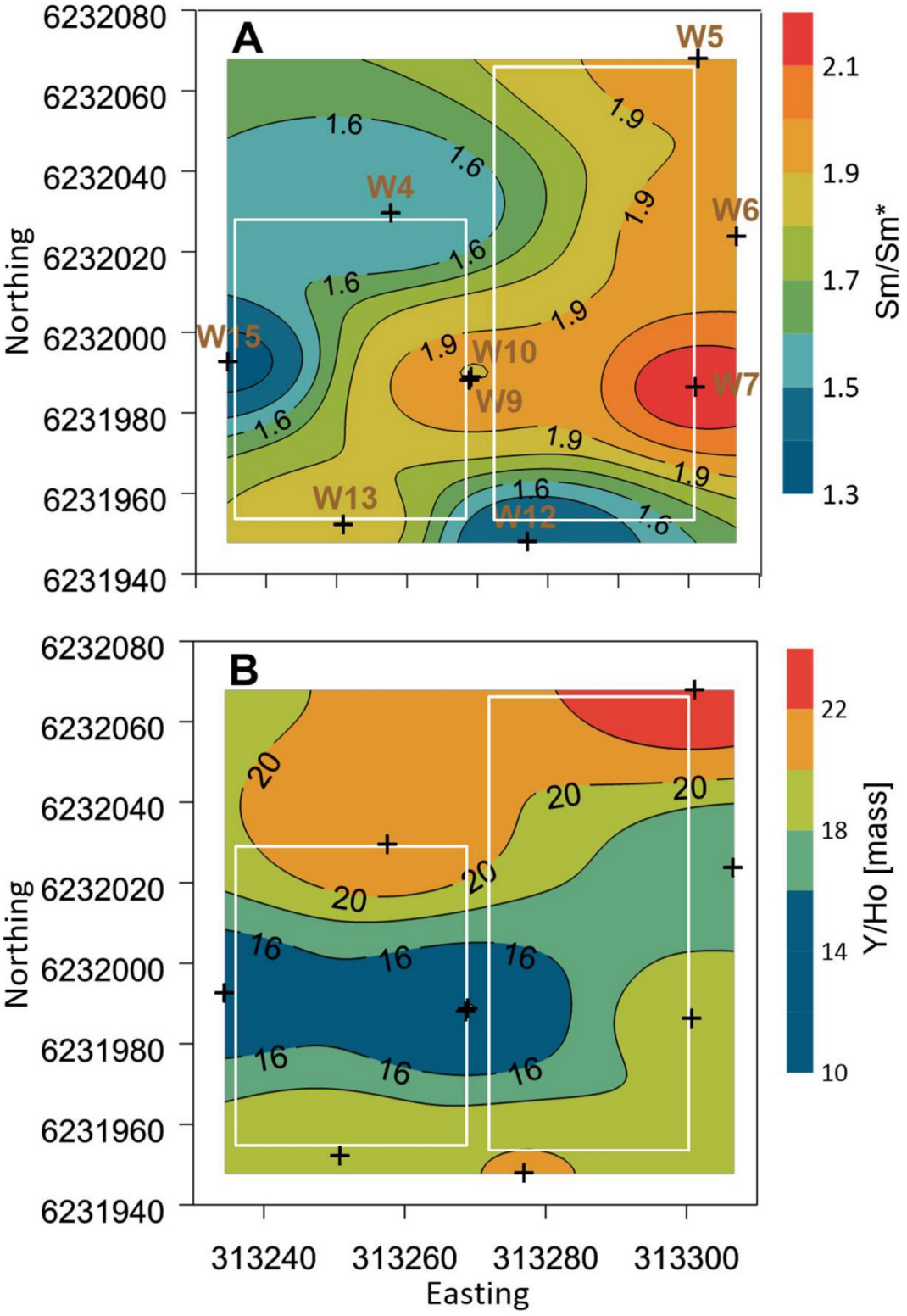

Fig. 7. A) Contour plot of Sm/Sm* anomalies (Table 1, Supplementary) across the trench area (white rectangles) showing position of monitoring wells used in contouring. B) Contour plot of Y/Ho ratios (Table 1, Supplementary), see Fig. 1 for detail positioning of monitoring wells. Note only W-series wells screening the top materials above the shale are used.

paths. This is particularly the case when investigating the dispersion and mobility of unconventional tracers like rare earth elements and yttrium. Despite REY's potential to fingerprint pollutant sources and processes, their similar behaviour to actinides, and their use in the nuclear industry, REY have seldom been used at the field-site scale of a low-level nuclear waste site. This paper covers that gap and shows the potential of REY to characterise similar sites as well as more prevalent landfill sites worldwide.

Rare earth elements and yttrium in groundwater can fingerprint sources of waste and/or geological materials, as well as processes along its flow path. REY groundwater near low-level waste is characterised by relatively

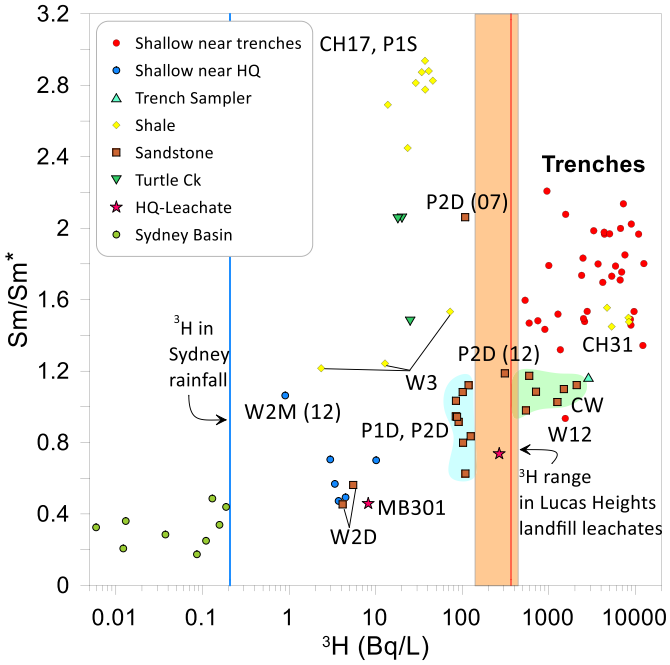

Fig. 8. Sm/Sm∗ anomaly ratios against ^{3}H (Bq L^{-1}). The vertical blue line is the average ^{3}H activity in Sydney rainfall (Peterson et al., 2020). The orange rectangle represents the range of ^{3}H data from neighbouring landfill leachate at Little Forest and the red line the mean value (Hughes et al., 2011). Some samples are labelled for reference; their locations can be seen in Fig. 1. Average multi-year ^{3}H groundwater activity at background sites (KMMA) are displayed for reference (Cendón et al., 2014).

high concentrations with specific distributions showing enrichments in Sm, Gd and Eu. This MREY enrichment is evident when concentrations are normalised against average upper crust compositions like PAAS. In the case of LFLS, groundwater near waste trenches shows REY distributions different to natural REY trends found in groundwater at background-regional sites within the same geology. Additionally, as NAA results show, neither local nor regional geological materials elsewhere in the Sydney Basin show any MREY enrichment that could justify the identified anomalies found in LFLS groundwater. Therefore, the unusual REY distributions found in LFLS groundwater around trenches and specifically enrichments in MREY, result from the disposal of low-level radioactive waste and subsequent water-waste-rock interactions.

Detailed groundwater REY analysis shows how samples have different REY normalised trends according to their location and distance from specific waste sources. The waste imprints the initial REY distribution and site hydrochemical conditions modify this along the flow path. The naturally low pH in LFLS groundwater minimises sorption into FeOOH and favours the retention of REY in solution, while the low availability of carbonate ions and seasonally high DOC concentrations favour the formation of REY-DOC complexes that follow recharged groundwater migrating laterally and, to a lesser extent, vertically. Fluctuations in pH and redox conditions with depth favour precipitation of FeOOH. This causes the scavenging of REY and constitutes a secondary chemical barrier to the transport of most REY and chemically similar actinides with depth.

The LFLS is surrounded by multiple sources of pollutants including an urban waste landfill. The normalised-REY distributions of landfill leachate, while lower in total concentration, are also characteristic and differ from those of groundwater near trenches. Landfill waste is directly in contact with the underlying sandstone, favouring the dispersion of pollutants via groundwater/leachate mixing. The strong chemical gradients away from the leachate collection system suggest sharp modifications to REY patterns in very short distances with Gd and Y anomalies developed and indicative of the landfill contributions. The differential behaviour of Gd and Y during FeOOH precipitation causes those elements to be relatively enriched in solution, with associated increases in yttrium concentration and Y/Ho ratios with depth. The differences observed between REY distributions in landfill and LFLS suggests REY can be an additional tool to trace mobility of pollutants in globally ubiquitous urban landfills.

CRediT authorship contribution statement

Experimental conceptualisation and design were carried out by DIC. Fieldwork and in-field geochemical analyses were conducted by DIC, JJH, SIH, BR and CEH. REY groundwater analysis was carried out by BR, DIC and HW. NAA was performed by AS. ITRAX analysis by PG. Data interpretation was primarily undertaken by DIC with contributions from CEH and TEP. The manuscript was written by DIC with input from all authors. Funding for the research was obtained by TEP.

Declaration of competing interest

The authors declare that they have no conflict of interest.

Acknowledgements

Thanks to Chris Dimovski, Sangeeth Thiruvoth and Kerry Wilsher from ANSTO for their constant logistical support, and the ANSTO Environmental Monitoring team who provide ongoing measurement of tritium in LFLS groundwater. Access to regional groundwater works and drill chips was facilitated by John Paul Williams from the NSW Department of Planning, Industry and Environment. Access to the cores BHF and LH2 was facilitated by the Londonderry Drillcore Library (NSW Resources and Geoscience). We also thank the editor and reviewers including Dr. Dennis Kraemer for very constructive reviews and comments.

Appendix A. Supplementary data

Supplementary data to this article can be found online at https://doi.org/10.1016/j.scitotenv.2022.154706.

References

Australian Atomic Energy Commission (AAEC), 1985. The little forest burial ground—an information paper. AAEC Report DR19. Environmental Science Division, Lucas Heights, NSW 27 pp.

Balboni, E., Simonetti, A., Spano, T., Cook, N.D., Burns, P.C., 2017. Rare-earth element fractionation in uranium ore and its U(VI) alteration minerals. Appl. Geochem. 87, 84–92. https://doi.org/10.1016/j.apgeochem.2017.10.007.

Bau, M., 1999. Scavenging of dissolved yttrium and rare earths by precipitating iron oxyhydroxide: experimental evidence for Ce oxidation, Y-ho fractionation, and lanthanide tetrad effect. Geochim. Cosmochim. Acta 63 (1), 67–77. https://doi.org/10.1016/S0016-7037(99)00014-9.

Bau, M., Dulski, P., 1996. Anthropogenic origin of positive gadolinium anomalies in river waters. Earth Planet. Sci. Lett. 143, 245–255.

Bayon, G., Birot, D., Bollinger, C., Barrat, J.A., 2011. Multi-element determination of trace elements in natural water reference materials by ICP-SFMS after Tm addition and iron co-precipitation. Geostand. Geoanal. Res. 35 (1), 145–153. https://doi.org/10.1111/j.1751-908X.2010.00064.x.

Bennett, J., 2008. Commissioning of NAA at the new OPAL reactor in Australia. J. Radioanal. Nucl. Chem. 278 (3), 671–673. https://doi.org/10.1007/s10967-008-1502-0.

Borrego, J., López-González, N., Carro, B., Lozano-Soria, O., 2004. Origin of the anomalies in light and middle REE in sediments of an estuary affected by phosphogypsum wastes (south-Western Spain). Mar. Pollut. Bull. 49 (11–12), 1045–1053. https://doi.org/10.1016/j.marpolbul.2004.07.009.

Bourg, S., Poinssot, C., 2017. Could spent nuclear fuel be considered as a non-conventional mine of critical raw materials? Prog. Nucl. Energy 94, 222–228. https://doi.org/10.1016/j.pnucene.2016.08.004.

Castañeda, S.S., Sucgang, R.J., Almoneda, R.V., Mendoza, N.D., David, C.P., 2012. Environmental isotopes and major ions for tracing leachate contamination from a municipal landfill in metro ManilaPhilippines. Journal of Environmental Radioactivity 110, 30–37. https://doi.org/10.1016/j.jenvrad.2012.01.022.

Cendón, D.I., Hankin, S.I., Williams, J.P., Van der Ley, M., Peterson, M., Hughes, C.E., Chisari, R., 2014. Groundwater residence time in a dissected and weathered sandstone plateau: kulnura-Mangrove Mountain aquifer, NSWAustralia. Australian Journal of Earth Sciences 61 (3), 475–499. https://doi.org/10.1080/08120099.2014.893628.

Cendón, D.I., Hughes, C.E., Harrison, J.J., Hankin, S.I., Johansen, M.P., Payne, T.E., Thiruvoth, S., 2015. Identification of sources and processes in a low-level radioactive

waste site adjacent to landfills: groundwater hydrogeochemistry and isotopes. Aust. J. Earth Sci. 62 (1), 123–141. https://doi.org/10.1080/08120099.2015.975155.
Coffey Partners International Pty Ltd, 1991. Little Forest, potential contaminated lands investigation west Menai—Stage 1. Report to NSW Department of Planning, Report No. E112/1– AC, Sydney, Australia.
Cozzarelli, I.M., Böhlke, J.K., Masoner, J., Breit, G.N., Lorah, M.M., Tuttle, M.L.W., Jaeschke, J.B., 2011. Biogeochemical evolution of a landfill leachate plume, NormanOklahoma. Ground Water 49 (5), 663–687. https://doi.org/10.1111/j.1745-6584.2010.00792.x.
Croudace, I.W., Rindby, A., Rothwell, R.G., 2006. ITRAX: description and evaluation of a new multi-function X-ray core scanner. Geol. Soc. Lond., Spec. Publ. 267 (1), 51. https://doi.org/10.1144/GSL.SP.2006.267.01.04.
Currie, L.A., 1968. Limits for qualitative detection and quantitative determinationApplication to radiochemistry. Analytical Chemistry 40, 586–593.
Dinali, G.S., Root, R.A., Amistadi, M.K., Chorover, J., Lopes, G., Guilherme, L.R.G., 2019. Rare earth elements (REY) sorption on soils of contrasting mineralogy and texture. Environ. Int. 128, 279–291. https://doi.org/10.1016/j.envint.2019.04.022.
Dulski, P., 1994. Interferences of oxide, hydroxide and chloride analyte species in the determination of rare earth elements in geological samples by inductively coupled plasma-mass spectrometry. Fresenius J. Anal. Chem. 350 (4–5), 194–203. https://doi.org/10.1007/bf00322470.
Duvert, C., Cendón, D.I., Raiber, M., Seidel, J.-L., Cox, M.E., 2015. Seasonal and spatial variations in rare earth elements to identify inter-aquifer linkages and recharge processes in an australian catchment. Chem. Geol. 396, 83–97. https://doi.org/10.1016/j.chemgeo.2014.12.022.
Ewing, R.C., 1999. Nuclear waste forms for actinides. Proc. Natl. Acad. Sci. 96 (7), 3432. https://doi.org/10.1073/pnas.96.7.3432.
Federal Register, 2018. Final list of critical minerals 2018. Federal Register 83 (97). https://www.federalregister.gov/documents/2018/05/18/2018-10667/final-list-of-critical-minerals-2018.
Geckeis, H., Rabung, T., 2008. Actinide geochemistry: from the molecular level to the real system. J. Contam. Hydrol. 102 (3), 187–195. https://doi.org/10.1016/j.jconhyd.2008.09.011.
Gutiérrez-Gutiérrez, S.C., Coulon, F., Jiang, Y., Wagland, S., 2015. Rare earth elements and critical metal content of extracted landfilled material and potential recovery opportunities. Waste Manag. 42, 128–136. https://doi.org/10.1016/j.wasman.2015.04.024.
Gutteridge Haskins & Davey Pty Ltd (GHD), 2003Gutteridge Haskins & Davey Pty Ltd (GHD) (2003). Additional Groundwater Contamination Assessment. Northern Boundary–Harrington's Quarry, Lucas Heights, NSW.
Hankin, S., 2012. Little forest burial ground- geology, geophysics and well installation (2009-2010). ANSTO Report E-781 182 pp.
Hathorne, E.C., Haley, B., Stichel, T., Grasse, P., Zieringer, M., Frank, M., 2012. Online preconcentration ICP-MS analysis of rare earth elements in seawater. geochemistryGeophysics, Geosystems 13 (1), Q01020.
Heim, C., Simon, K., Ionescu, D., Reimer, A., De Beer, D., Quéric, N.-V., Thiel, V., 2015. Assessing the utility of trace and rare earth elements as biosignatures in microbial iron oxyhydroxides. FrontiersEarth Sci. 3 (6). https://doi.org/10.3389/feart.2015.00006.
Hissler, C., Stille, P., Iffly, J.F., Guignard, C., Chabaux, F., Pfister, L., 2016. Origin and dynamics of rare earth elements during flood events in Contaminated River basins: Sr–Nd–Pb isotopic evidence. Environ. Sci. Technol. 50 (9), 4624–4631. https://doi.org/10.1021/acs.est.5b03660.
Hughes, C.E., Cendón, D.I., Harrison, J.J., Hankin, S.I., Collins, R.N., Payne, T.E., Loosz, T., 2011. Movement of a tritium plume in shallow groundwater at a legacy low level radioactive waste disposal site in eastern Australia. J. Environ. Radioact. 102, 943–952.
ILLWD, 2011. International low-level waste disposal practices and facilities. Accessed online September 2021Fuel Cycle Research and Development. U.S. Department of Energy ANL-FCT-324 . https://publications.anl.gov/anlpubs/2011/12/71232.pdf.
Isaacs, S.R., Mears, K.F., 1977. A study of the burial ground used for radioactive waste at the Little Forest area near Lucas Heights New South Wales. Australian Atomic Energy Commission, AAEC Report E427, Lucas Heights, NSW , p. 50. https://apo.ansto.gov.au/dspace/handle/10238/644.
Isnard, H., Brennetot, R., Caussignac, C., Caussignac, N., Chartier, F., 2005. Investigations for determination of Gd and Sm isotopic compositions in spent nuclear fuels samples by MC ICPMS. Int. J. Mass Spectrom. 246 (1), 66–73. https://doi.org/10.1016/j.ijms.2005.08.008.
Iwashita, M., Saito, A., Arai, M., Furusho, Y., Shimamura, T., 2011. Determination of rare earth elements in rainwater collected in suburban Tokyo. Geochem. J. 45, 187–197.
Johannesson, K.H. (Ed.), 2005. Rare Earth Elements in Groundwater Flow Systems. Water Science and Technology Library v 51. Springer, The Netherlands.
Johannesson, K.H., Stetzenbach, J.J., 1995. Speciation of the rare earth element neodymium in groundwates of the Nevada test site and Yucca Mountain and implications for actinide solubility. Appl. Geochem. 10, 565–572.
Johannesson, K.H., Stetzenbach, K.J., Hodge, V.F., 1997. Rare earth elements as geochemical tracers of regional groundwater mixing. Geochim. Cosmochim. Acta 61 (17), 3605–3618. https://doi.org/10.1016/S0016-7037(97)00177-4.
Kawabe, I., Ohta, A., Ishii, S., Tokumura, M., Miyauchi, K., 1999. REE partitioning between Fe-Mn oxyhydroxide precipitates and weakly acid NaCl solutions: convex tetrad effect and fractionation of Y and Sc from heavy lanthanides. Geochem. J. 33, 167–179.
Knappe, A., Möller, P., Dulski, P., Pekdeger, A., 2005. Positive gadolinium anomaly in surface water and ground water of the urban area BerlinGermany. Geochemistry 65 (2), 167–189. https://doi.org/10.1016/j.chemer.2004.08.004.
Krauskopf, K.B., 1986. Thorium and rare-earth metals as analogs for actinide elements. Chem. Geol. 55 (3), 323–335. https://doi.org/10.1016/0009-2541(86)90033-1.
Lawrence, M.G., Kamber, B.S., 2007. Rare earth element concentrations in the natural water reference materials (NRCC) NASS-5, CASS-4 and SLEW-3. Geostand. Geoanal. Res. 31 (2), 95–103. https://doi.org/10.1111/j.1751-908X.2007.00850.x.
Lawrence, M., Greig, A., Collerson, K., Kamber, B., 2006. Rare earth element and yttrium variability in south East Queensland waterways. Aquat. Geochem. 12 (1), 39–72. https://doi.org/10.1007/s10498-005-4471-8.
Leybourne, M.I., Johannesson, K.H., 2008. Rare earth elements (REE) and yttrium in stream waters, stream sediments, and Fe–Mn oxyhydroxides: fractionation, speciation, and controls over REE + Y patterns in the surface environment. Geochim. Cosmochim. Acta 72 (24), 5962–5983. https://doi.org/10.1016/j.gca.2008.09.022.
Liu, H., Pourret, O., Guo, H., Bonhoure, J., 2017. Rare earth elements sorption to iron oxyhydroxide: model development and application to groundwater. Appl. Geochem. 87, 158–166. https://doi.org/10.1016/j.apgeochem.2017.10.020.
Loell, M., Reiher, W., Felix-Henningsen, P., 2011. Contents and bioavailability of rare earth elements in agricultural soils in Hesse (Germany). J. Plant Nutr. Soil Sci. 174, 644–654.
McCarthy, J.F., Sanford, W.E., Staffford, P.L., 1998. Lanthanide field tracers demonstrate enhanced transport of transuranic radionuclides by natural organic matter. Environ. Sci. Technol. 32, 3901–3906.
McCarthy, J.F., Czerwinski, K.R., Sanford, W.E., Jardine, P.M., Marsh, J.D., 1998a. Mobilization of transuranic radionuclides from disposal trenches by natural organic matter. J. Contam. Hydrol. 30 (1), 49–77. https://doi.org/10.1016/S0169-7722(97)00032-6.
McKibbin, D., Smith, P.C., 2000. Sandstone hydrogeology of the Sydney region. In: Franklin, B.J., McNally, G.H. (Eds.), Sandstone City, Sydney's Dimension Stone and Other Sandstone Geomaterials. Monograph No 5. Geological Society of Australia Environmental, Engineering and Hydrogeology Specialist Group, Sydney NSW.
Missana, T., Alonso, Ú., García-Gutiérrez, M., Mingarro, M., 2008. Role of bentonite colloids on europium and plutonium migration in a granite fracture. Appl. Geochem. 23 (6), 1484–1497. https://doi.org/10.1016/j.apgeochem.2008.01.008.
Möller, P., Bau, M., 1993. Rare-earth patterns with positive cerium anomaly in alkaline waters from Lake VanTurkey. Earth and Planetary Science Letters 117 (3–4), 671–676. https://doi.org/10.1016/0012-821X(93)90110-U.
Möller, P., Paces, T., Dulski, P., Morteani, G., 2002. Anthropogenic gd in surface water, drainage system, and the water supply of the City of PragueCzech Republic. Environmental Science & Technology 36 (11), 2387–2394. https://doi.org/10.1021/es010235q.
Möller, P., Rosenthal, E., Dulski, P., Geyer, S., Guttman, Y., 2003. Rare earths and yttrium hydrostratigraphy along the Lake kinneret-Dead Sea–Arava transform faultIsrael and adjoining territories. Applied Geochemistry 18 (10), 1613–1628. https://doi.org/10.1016/S0883-2927(03)00044-1.
Möller, P., Dulski, P., Salameh, E., Geyer, S., 2006. Characterization of the sources of thermal spring- and well water in Jordan by rare earth element and yttrium distribution and stable isotopes of H2O. Acta Hydrochim. Hydrobiol. 34 (1–2), 101–116. https://doi.org/10.1002/aheh.200500614.
Nance, W.B., Taylor, S.R., 1976. Rare earth element patterns and crustal evolution—I. Australian post-Archean sedimentary rocks. Geochim. Cosmochim. Acta 40 (12), 1539–1551. https://doi.org/10.1016/0016-7037(76)90093-4.
Nozaki, Y., Zhang, J., Amakawa, H., 1997. The fractionation between Y and ho in the marine environment. Earth Planet. Sci. Lett. 148 (1–2), 329–340.
Olivarez, A.M., Owen, R.M., 1991. The europium anomaly of seawater: implications for fluvial versus hydrothermal REE inputs to the oceans. Chem. Geol. 92, 317–328.
Pack, A., Russell, S.S., Shelley, J.M.G., van Zuilen, M., 2007. Geo- and cosmochemistry of the twin elements yttrium and holmium. Geochim. Cosmochim. Acta 71 (18), 4592–4608. https://doi.org/10.1016/j.gca.2007.07.010.
Payne, T.E., 2012. Background Report on the Little Forest Burial Ground Legacy Waste Site (ANSTO/E-780). Accessed onlineAustralian Nuclear Science and Technology Organisation, Lucas Heights, NSW. https://apo.ansto.gov.au/dspace/handle/10238/4473.
Payne, T.E., Harrison, J.J., Hughes, C.E., Johansen, M.P., Thiruvoth, S., Wilsher, K.L., Zawadzki, A., 2013. Trench 'Bathtubbing' and surface plutonium contamination at a legacy radioactive waste site. Environ. Sci. Technol. 47 (23), 13284–13293. https://doi.org/10.1021/es403278r.
Payne, T.E., Harrison, J.J., Cendon, D.I., Comarmond, M.J., Hankin, S., Hughes, C.E., Wilsher, K.L., 2020. Radionuclide distributions and migration pathways at a legacy trench disposal site. J. Environ. Radioact. 211, 106081. https://doi.org/10.1016/j.jenvrad.2019.106081.
Peters, J.A., Djanashvili, K., Geraldes, C.F.G.C., Platas-Iglesias, C., 2020. The chemical consequences of the gradual decrease of the ionic radius along the Ln-series. Coord. Chem. Rev. 406, 213146. https://doi.org/10.1016/j.ccr.2019.213146.
Peterson, M.A., Cendón, D.I., Crawford, J., Hughes, C.E., Meredith, K., Hankin, S., Dimovski, C., 2020. TLRP5: Environmental isotopes investigations into periodic and recent water losses from Thirlmere Lakes. A Report to the NSW Department of Planning, Industry and Environment. ANSTO/C-1690 68 pp + appendices.
Pourmand, A., Dauphas, N., Ireland, T.J., 2012. A novel extraction chromatography and MC-ICP-MS technique for rapid analysis of REE, Sc and Y: revising CI-chondrite and post-Archean Australian shale (PAAS) abundances. Chem. Geol. 291, 38–54. https://doi.org/10.1016/j.chemgeo.2011.08.011.
Pourret, O., Davranche, M., Gruau, G., Dia, A., 2007. Rare earth elements complexation with humic acid. Chem. Geol. 243 (1–2), 128–141. https://doi.org/10.1016/j.chemgeo.2007.05.018.
Ray, W.E., 1971. The lanthanons as nuclear control materials. Nucl. Eng. Des. 17 (3), 377–396. https://doi.org/10.1016/0029-5493(71)90100-2.
Robinson, H.D., Gronow, J.R., 1996. Tritium levels in leachates and condensates from domestic wastes in landfill sites. Water Environ. J. 10 (6), 391–398. https://doi.org/10.1111/j.1747-6593.1996.tb00070.x.
Rogowska, J., Olkowska, E., Ratajczyk, W., Wolska, L., 2018. Gadolinium as a new emerging contaminant of aquatic environments. Environ. Toxicol. Chem. 37 (6), 1523–1534. https://doi.org/10.1002/etc.4116.
Rousseau, T.C.C., Sonke, J.E., Chmeleff, J., Candaudap, F., Lacan, F., Boaventura, G., Seyler, P., Jeandel, C., 2013. Rare earth element analysis in natural waters by multiple isotope dilution – sector field ICP-MS. J. Anal. At. Spectrom. 28 (4), 573–584. https://doi.org/10.1039/C3JA30332B.

Rowling, B., Kinsela, A.S., Comarmond, M.J., Hughes, C.E., Harrison, J.J., Johansen, M.P., Payne, T.E., 2017. Measurement of tributyl phosphate (TBP) in groundwater at a legacy radioactive waste site and its possible role in contaminant mobilisation. J. Environ. Radioact. 178–179, 377–384. https://doi.org/10.1016/j.jenvrad.2017.05.015.

Rudnick, R.L., Gao, S., Heinrich, D.H., Karl, K.T., 2003. Composition of the continental crust. Treatise on Geochemistry. Pergamon, Oxford, pp. 1–64.

Stolpe, B., Guo, L., Shiller, A.M., 2013. Binding and transport of rare earth elements by organic and iron-rich nanocolloids in Alaskan rivers, as revealed by field-flow fractionation and ICP-MS. Geochim. Cosmochim. Acta 106, 446–462. https://doi.org/10.1016/j.gca.2012.12.033.

Tang, J., Johannesson, K.H., 2006. Controls on the geochemistry of rare earth elements along a groundwater flow path in the Carrizo sand aquifer, Texas, USA. Chem. Geol. 225 (1), 156–171. https://doi.org/10.1016/j.chemgeo.2005.09.007.

Tang, J., Johannesson, K.H., 2010. Rare earth elements adsorption onto Carrizo sand: influence of strong solution complexation. Chem. Geol. 279 (3–4), 120–133. https://doi.org/10.1016/j.chemgeo.2010.10.011.

Tweed, S.O., Weaver, T.R., Cartwright, I., Schaefer, B., 2006. Behavior of rare earth elements in groundwater during flow and mixing in fractured rock aquifers: an example from the Dandenong ranges, Southeast Australia. Chem. Geol. 234 (3–4), 291–307. https://doi.org/10.1016/j.chemgeo.2006.05.006.

Vermeire, M.-L., Cornu, S., Fekiacova, Z., Detienne, M., Delvaux, B., Cornélis, J.-T., 2016. Rare earth elements dynamics along pedogenesis in a chronosequence of podzolic soils. Chem. Geol. 446, 163–174. https://doi.org/10.1016/j.chemgeo.2016.06.008.

Whittem, R.N., 1968. Determination of the thermal neutron capture cross section of Samarium-148 (AAEC/TM443). Australian Atomic Energy Commission, Lucas Heights, NSW.

Wray, R.A., 1995. Solutional Landforms in Quartz Sandstones of the Sydney Basin. 399 ppUniversity of Wollongong. http://ro.uow.edu.au/theses/1981.

Wyndham, T., McCulloch, M.T., Fallon, S., Alibert, C., 2004. High-resolution coral records of rare earth elements in coastal seawater: biogeochemical cycling and a new environmental proxy. Geochim. Cosmochim. Acta 68 (9), 2067–2080.

Yeghicheyan, D., Bossy, C., Bouhnik Le Coz, M., Douchet, C., Granier, G., Heimburger, A., Sonke, J.E., 2013. A compilation of silicon, rare earth element and twenty-one other trace element concentrations in the Natural River water reference material SLRS-5 (NRC-CNRC). Geostand. Geoanal. Res. 37 (4), 449–467. https://doi.org/10.1111/j.1751-908X.2013.00232.x.